



UNIVERSITI PUTRA MALAYSIA

***AEROELASTIC FLUTTER PERFORMANCE OF SHAPE MEMORY
ALLOY EMBEDDED 3D WOVEN COMPOSITE PLATE UNDER
SUBSONIC FLOW***

DANISH MAHMOOD BAITAB

FK 2021 71



**AEROELASTIC FLUTTER PERFORMANCE OF SHAPE MEMORY ALLOY-
EMBEDDED 3D WOVEN COMPOSITE PLATE UNDER SUBSONIC FLOW**

By

DANISH MAHMOOD BAITAB

**Thesis Submitted to the School of Graduate Studies, Universiti Putra
Malaysia, in Fulfilment of the Requirements for the Degree of Doctor of
Philosophy**

March 2021

All material contained within the thesis, including without limitation text, logos, icons, photographs and all other artwork, is copyright material of Universiti Putra Malaysia unless otherwise stated. Use may be made of any material contained within the thesis for non-commercial purposes from the copyright holder. Commercial use of material may only be made with the express, prior, written permission of Universiti Putra Malaysia.

Copyright © Universiti Putra Malaysia



Abstract of thesis presented to the Senate of Universiti Putra Malaysia in
fulfilment of the requirement for the degree of Doctor of Philosophy

AEROELASTIC FLUTTER PERFORMANCE OF SHAPE MEMORY ALLOY- EMBEDDED 3D WOVEN COMPOSITE PLATE UNDER SUBSONIC FLOW

By

DANISH MAHMOOD BAITAB

March 2021

**Chair : Assoc. Prof. Dayang Laila binti Abang Haji Abdul
Majid, PhD**
Faculty : Engineering

Recent advancements in the aeroelasticity of aircraft structures show an increasing trend in using smart materials with composite structures for improved aeroelastic performance. An example is using shape memory alloys (SMAs) to be combined with composite structures either as actuators or for morphing capabilities. SMA has the ability to accommodate strain rather than breakage by unfolding its lattice when a load is applied and also, it generates stresses due to phase transformation from martensite to austenite at higher temperatures. Due to this coupling effect of SMAs in response to load and temperature, SMAs are embedded in laminated composites for improving damping, stiffness and vibrational characteristics. However, SMA embedded laminated composites are poor in through-the-thickness mechanical properties and SMA-induced stresses and temperature can cause delamination of plies that ultimately results in structural failures under high vibrations.

In this research, SMA wires are embedded in the glass-fibre reinforced composites using 3D woven reinforcements to improve tensile and vibrational characteristics. 3D woven reinforcements provides delamination resistance, higher through-the-thickness mechanical properties and a strong grip to SMA wire due to binding yarns of 3D structure in through-the-thickness direction. Three different 3D woven orthogonal interlock configurations having different interlocking pattern of yarns with SMA wire are analysed in terms of tensile, dynamic and aeroelastic flutter properties. These 3D configurations are layer-to-layer (L2L), through-the-thickness (TT), and a modified interlock (MF) structure that provides the strongest grip to SMA wire than L2L and TT. SMA positioning was also evaluated for both dynamic and aeroelastic flutter properties i.e. SMA at mid, near to trailing, and near to leading edge of cantilevered composite plate.

Tensile results showed that embedding SMA wires into structures have significantly improved tensile properties due to the coupling effect of SMA. The vibrational characteristics are also improved by embedding SMA wire and SMA wire at mid has a higher impact on bending mode frequencies while torsional mode frequencies are more affected for SMA wire at near to trailing and leading edge. Interesting results are obtained from aeroelastic testing by wind tunnel test. Activating SMA results in decrement of flutter speed and flutter frequency due to increment in flexibility of the deflected plate in airflow by SMA-induced stresses. However, there is an improvement in post-flutter behavior as the bending and twist limit cycle oscillation (LCO) amplitudes are reduced by activating SMA wire.

Among 3D configurations, L2L displayed the highest increase of 34.9% in Young's modulus as L2L provides more freedom to SMA for generating stresses due to loose grip of yarns to SMA. For dynamic properties, L2L with SMA at mid showed the highest percentage increment of 17%, 11% and 4% in natural frequencies of first three bending modes respectively. For post-flutter behavior, L2L with SMA near to trailing edge showed a significant decrement of 22.2% in twist LCO amplitude while L2L with SMA at mid showed a decrement of 9.5% for bending LCO amplitude. Hence, this work showed that embedding SMA is beneficial for improving tensile and dynamic properties as well as mitigating the post-flutter vibrations but as the consequence of reduced flutter speed and frequency.

Abstrak tesis yang dikemukakan kepada Senat Universiti Putra Malaysia sebagai memenuhi keperluan untuk ijazah Doktor Falsafah

PRESTASI AEROELASTIK KIBARAN ALOI MEMORI BENTUK YANG TERBENAM DALAM PLAT KOMPOSIT TENUNAN 3D DI BAWAH ALIRAN SUBSONIK

Oleh

DANISH MAHMOOD BAITAB

Mac 2021

Pengerusi : Prof. Madya Dayang Laila binti Abang Haji Abdul Majid, PhD
Fakulti : Kejuruteraan

Perkembangan terkini dalam struktur aeroelastik pesawat menunjukkan aliran peningkatan dari segi penggunaan bahan pintar dalam struktur komposit untuk meningkatkan prestasi aeroelastik. Contohnya melalui penggunaan bahan aloi memori bentuk (SMA) yang digabungkan dengan struktur komposit sama ada sebagai penggerak atau untuk keupayaan gabungan. SMA memiliki kemampuan untuk menampung terikan berbanding pemecahan dengan merungkaikan kekisi ketika beban dikenakan dan juga menghasilkan tekanan akibat transformasi fasa daripada martensit ke austenit pada suhu yang lebih tinggi. Disebabkan kesan gandingan SMA ini hasil tindak balas terhadap beban dan suhu, SMA yang terbenam dalam komposit berlapis berupaya meningkatkan ciri redaman, kekukuhan dan getaran. Walau bagaimanapun, SMA terbenam dalam komposit berlapis lemah dari segi sifat mekanikal dalam arah ketebalan serta perubahan tekanan dan suhu yang didorong oleh SMA juga akan menyebabkan pemisahan lapisan yang akhirnya mengakibatkan kegagalan struktur di bawah getaran tinggi.

Dalam penyelidikan ini, dawai SMA terbenam dalam komposit bertetulang gentian kaca menggunakan tetulang tenunan 3D dikaji untuk meningkatkan ciri tegangan dan getaran. Tetulang tenunan 3D memberikan ketahanan nyah-lapisan, sifat mekanik yang lebih tinggi merentasi ketebalan dan genggam kuat pada dawai SMA kerana adanya pengikat benang struktur 3D mengikut arah ketebalan. Tiga konfigurasi tenunan 3D dengan ciri ortogonal saling-mengunci yang berbeza dimana setiapnya mempunyai corak benang saling-mengunci dengan wayar SMA yang berlainan akan dianalisis dari segi sifat tegangan, dinamik dan aeroelastik. Konfigurasi 3D ini terdiri daripada lapisan ke lapisan (L2L), arah ketebalan (TT), dan struktur saling-mengunci yang diubahsuai (MF) yang memberikan genggam terkuat pada dawai SMA

berbanding dengan L2L dan TT. Kedudukan SMA juga dinilai dari segi sifat kibar dinamik dan aeroelastik, contohnya; SMA pada kedudukan tengah, dekat dengan pinggir mengekor, dan dekat dengan pinggir depan plat komposit julur.

Keputusan tegangan menunjukkan bahawa pembenaman dawai SMA ke dalam struktur meningkatkan sifat tegangan dengan ketara kerana kesan gandingan SMA. Ciri getaran juga diperbaiki dengan membenamkan dawai SMA dan dawai SMA pada kedudukan tengah mempunyai hentaman tinggi pada frekuensi mod lenturan, manakala frekuensi mod kilasan lebih banyak dipengaruhi oleh dawai SMA pada jarak dekat dengan pinggir mengekor dan dekat dengan pinggir depan. Keputusan yang menarik diperolehi daripada pengujian aeroelastik melalui ujian terowong angin. Pengaktifan SMA menyebabkan susutan kelajuan kibar dan frekuensi kibar kerana tekanan yang disebabkan oleh SMA meningkatkan fleksibiliti plat terpesong dalam aliran udara. Walau bagaimanapun, terdapat peningkatan dalam kelakuan pasca-kibar disebabkan had lenturan dan puncak piuh litar ayunan (LCO) yang dikurangkan melalui pengaktifan dawai SMA.

Di antara konfigurasi 3D, L2L memaparkan peningkatan tertinggi sebanyak 34.9% dalam modulus Young kerana L2L memberikan lebih banyak kebebasan kepada SMA untuk menghasilkan tekanan disebabkan genggaman benang yang longgar ke atas SMA. Dari segi sifat dinamik, L2L bersama SMA pada kedudukan tengah menunjukkan peningkatan peratusan tertinggi iaitu, sebanyak 17%, 11% dan 4% masing-masing pada frekuensi semula jadi berasaskan tiga mod lenturan pertama. Bagi kelakuan pasca-kibar, L2L bersama SMA dekat dengan pinggir mengekor menunjukkan penurunan ketara sebanyak 22.2% pada puncak piuh litar ayunan (LCO) manakala L2L bersama SMA pada kedudukan tengah menunjukkan penurunan sebanyak 9.5% untuk puncak lenturan litar ayunan (LCO). Oleh itu, hasil kajian ini menunjukkan bahawa pembenaman SMA bermanfaat untuk meningkatkan sifat tegangan dan dinamik serta mengurangkan getaran pasca-kibar tetapi sebagai akibat penurunan kelajuan serta frekuensi kibar.

ACKNOWLEDGEMENTS

I would like to express my special thanks of gratitude to my main supervisor, Dr. Dayang Laila Abang Abdul Majid for her constant support and guidance throughout my journey of completing this thesis. Doing research under her supervision gave me various opportunities and experiences in the research and academics field, which I believe will greatly benefit my career and myself in the future. My gratitude also goes to the supervisory committee members, Dr. Ermira Junita Abdullah and Dr. Mohd Faisal Abdul Hamid for all the support.

My gratitude also goes to all supporting lab technicians, especially Mr. Ahmad Saifol, Mr. Mohd Azfar Roslan, Mr. Saffairus Salih, and Mr. Mohd Suhardi (Aerospace Engineering) for assisting my fabrication and experimental work.

Lastly, I want to express my gratitude to all families and friends that had been endlessly supporting my PhD journey. My special thanks to my parents, my wife, my son and siblings for their moral and financial support.

This thesis was submitted to the Senate of Universiti Putra Malaysia and has been accepted as fulfilment of the requirement for the degree of Doctor of Philosophy. The members of the Supervisory Committee were as follows:

Dayang Laila binti Abang Haji Abdul Majid, PhD

Associate Professor
Faculty of Engineering
Universiti Putra Malaysia
(Chairman)

Ermira Junita binti Abdullah, PhD

Senior Lecturer
Faculty of Engineering
Universiti Putra Malaysia
(Member)

Mohd Faisal bin Abdul Hamid, PhD

Senior Lecturer
Faculty of Engineering
Universiti Putra Malaysia
(Member)

ZALILAH MOHD SHARIFF, PhD

Professor and Dean
School of Graduate Studies
Universiti Putra Malaysia

Date: 12 August 2021

TABLE OF CONTENTS

	Page
ABSTRACT	i
ABSTRAK	iii
ACKNOWLEDGEMENTS	v
APPROVAL	vi
DECLARATION	viii
LIST OF TABLES	xiii
LIST OF FIGURES	xv
LIST OF ABBREVIATIONS	xx
CHAPTER	
1 INTRODUCTION	1
1.1 Introduction	1
1.2 Problem Statement	3
1.3 Research Objectives	4
1.4 Scope of Research	4
1.5 Thesis Outline	5
2 LITERATURE REVIEW	6
2.1 Aeroelasticity	6
2.1.1 Flutter	8
2.1.2 Aeroelastic Flutter Analysis	10
2.2 Composite Structures in Aircrafts	15
2.2.1 Woven Composites	16
2.2.2 Importance of 3D Reinforced Composites	23
2.3 Smart Materials	24
2.3.1 Shape Memory Alloys (SMAs)	26
2.4 Embedding SMA Wires into Composites	29
2.4.1 Objectives of Embedding SMA Wires into Composites	29
2.4.2 Factors Considered for Embedding SMA Wires into Composites	30
2.4.3 Techniques for Embedding SMA Wires into Composites	32
2.5 Passive and Active Tailoring of Composites for Improving Aeroelastic Performance	44
2.5.1 Passive Tailoring of Composites	44
2.5.2 Active Tailoring of Composites by Embedding Shape Memory Alloys	47
2.6 Chapter Summary	53

3	METHODOLOGY	54
3.1	Materials	56
3.1.1	Force Temperature Calibration of SMA Wire	58
3.2	Woven Structures	59
3.2.1	Woven Structures with Embedded SMA Wires	61
3.3	Manufacturing	63
3.3.1	2D and 3D Weaving of Glass Fabric Reinforcements	63
3.3.2	Composite Fabrication of 2D Plain Woven and 3D Woven Structures	67
3.4	Determination of Volume Fraction of Constituents in 2D Laminated and 3D Woven Composites	68
3.5	Tensile Test	69
3.5.1	Preparation of Samples for Tensile Test	70
3.5.2	Experimental Setup for Tensile Test	70
3.6	Modal Test	73
3.6.1	Test Sample Preparation	74
3.6.2	Experimental Setup for Modal Analysis	75
3.6.3	Verification of Impact Hammer Test with Analytical and Computational Method	76
3.7	Aeroelastic Flutter Test	77
3.7.1	Experimental Setup for Wind Tunnel Flutter Testing	78
3.7.2	The Bending Moment and Deflection of Composite Plate under Airflow and SMA-Induced Stresses	84
3.8	Chapter Summary	86
4	RESULTS AND DISCUSSION	88
4.1	Volume Fraction of Constituents in 2D laminated and 3D Composite Structures	88
4.2	Tensile Results	89
4.2.1	Activation Temperature of SMA wire for Tensile Test	90
4.2.2	2D Plain Woven Laminated Composites	91
4.2.3	3D Orthogonal Layer-to-Layer (L2L) Interlock Composites	93
4.2.4	3D Orthogonal Through-the-Thickness (TT) Interlock Composites	95
4.2.5	3D Orthogonal Modified (MF) Interlock Composites	96
4.2.6	Tensile Properties Affected by Embedded SMA Wire and 3D Yarn Pattern	98

4.2.7	Failure Modes of 3D Structures under Tensile Test	102
4.3	Modal Analysis Results	105
4.3.1	Verification of Experimental Modal Testing with Analytical and Computational Method	106
4.3.2	Natural Frequencies of 3D Woven Layer-to-Layer Interlock Composite Plates	108
4.3.3	Natural Frequencies of 3D Woven Through-the-Thickness Interlock Composite Plates	112
4.3.4	Natural Frequencies of 3D Woven Modified Interlock Composite Plates	113
4.3.5	Modal Properties Affected by Embedded SMA Wire and 3D Yarn Pattern	115
4.4	Aeroelastic Analysis Results	116
4.4.1	Aeroelastic behavior of 3D Woven Layer-to-Layer Interlock Composite Plates	116
4.4.2	Aeroelastic behavior of 3D Woven Through-the-Thickness Composite Plates	123
4.4.3	Aeroelastic behavior of 3D Woven Modified Interlock Composite Plates	127
4.4.4	Effect of SMA Positioning and 3D Configurations on Aeroelastic Performance of Composite Plate	131
4.5	Chapter Summary	133
5	CONCLUSION AND RECOMMANDATIONS	135
5.1	Conclusion	135
5.2	Recommendations for Future Work	136
	REFERENCES	138
	APPENDICES	155
	BIODATA OF STUDENT	165
	LIST OF PUBLICATIONS	166

LIST OF TABLES

Table		Page
2.1	Summary of previous work on embedding SMA wires in between laminates of composites	35
2.2	Summary of previous work on embedding SMA wires directly into matrix	39
2.3	Summary of previous work on embedding SMA woven structures into composites	43
2.4	Summary of previous work on embedding SMA wires in composite structures for improving flutter properties	50
3.1	Properties of E-glass fibre yarn	56
3.2	Properties of matrix	56
3.3	Properties of SMA wire	57
3.4	Plain woven and 3D woven structures with and without SMA wires	62
3.5	Position of SMA wire (span-wise) for modal analysis and flutter test	65
3.6	Equipment used for impact hammer modal testing	74
4.1	Fibre, matrix, and void volume fraction (%) in 2D laminated and 3D woven composites	89
4.2	Tensile properties of 2D plain woven laminated composites	92
4.3	Tensile properties of 3D orthogonal L2L interlock structures	94
4.4	Tensile properties of 3D orthogonal TT interlock structures	96
4.5	Tensile properties of 3D modified orthogonal structure	98
4.6	Comparison of mode shapes of natural frequencies of aluminium plate obtained from impact hammer test and MSC Nastran	107

4.7	Comparison of natural frequencies of Aluminium plate obtained from impact hammer test with FEA and numerical results	108
4.8	Mode Shapes of 3D Layer-to-Layer interlock composite plate obtained from impact hammer test	109
4.9	Natural frequencies of L2L without SMA wire, SMA wire at mid (inactive and active), near to trailing edge (inactive and active), and near to leading edge (inactive and active)	110
4.10	Natural frequencies of TT without SMA wire, SMA wire at mid (inactive and active), trailing edge (inactive and active) and leading edge (inactive and active)	112
4.11	Natural frequencies of MF without SMA wire, SMA wire at mid (inactive and active), near to trailing edge (inactive and active) and near to leading edge (inactive and active)	114
4.12	The percentage increment in bending moments of 3D L2L, TT, and MF by activated SMA wire at mid, trailing, and leading edge	120
4.13	Flutter properties of 3D woven Layer-to-Layer interlock composite plates	123
4.14	Flutter properties of 3D woven through-the-thickness interlock composite plates	127
4.15	Flutter properties of 3D woven modified interlock composite plates	131

LIST OF FIGURES

Figure		Page
2.1	Collar's Triangle	7
2.2	Modes of vibration for one-dimensional cantilever beam	10
2.3	Aeroelastic Feedback diagram	12
2.4	3D woven structures	18
2.5	3D woven multilayer (a) Orthogonal interlock (b) Angle interlock	18
2.6	(a) 3D woven through-the-thickness interlock (b) 3D woven layer-to-layer interlock	19
2.7	Types of Multilayer 3D woven structure	20
2.8	(a) Loose woven triaxial fabric (b) Tight woven triaxial fabric	20
2.9	Process of triaxial weaving	21
2.10	The orthogonal woven unit cell	21
2.11	3D Orthogonal weaving	22
2.12	3D woven angle interlock structures (a) Layer-to-Layer (b) Through-the-Thickness	22
2.13	3D angle interlock weaving	23
2.14	(a) SMA austenite phase (well packed crystalline structure) (b) SMA martensite phase (loosely packed crystalline structure)	27
2.15	Shape memory effect	28
2.16	Pseudoelastic effect	29
2.17	SMA wires embedded between laminate layers	32
2.18	SMA wires embedded as reinforcement	37

2.19	(a) SMA wires in weft direction interwoven with warp yarns (b) SMA and yarns in weft direction interwoven with warp yarns (c) SMA woven mesh (Warp and weft are SMA wires)	41
3.1	Flow chart of research methodology	55
3.2	DSC results for SMA wire	57
3.3	a) Experimental assembly for temperature-force calibration of SMA wire (b) Schematic diagram for temperature-force calibration of SMA wire	58
3.4	SMA temperature-force calibration results	59
3.5	Detailed flow chart of research work	60
3.6	Cross-sectional and 3D views of (a) 3D orthogonal layer-to-layer interlock structure (b) 3D orthogonal through-the-thickness interlock structure (c) 3D orthogonal modified interlock structure	61
3.7	Warping process	63
3.8	Weave designs and cross-sectional views of 2D plain woven and 3D woven structures	64
3.9	SMA wires are inserted into the middle layer of structures at a distance of 30mm during 3D weaving	65
3.10	The Position of SMA wire in Plate-like wing (span-wise) (a) At mid (b) Near to trailing edge (c) Near to leading edge	66
3.11	3D weaving of composite plate for evaluating dynamic and aeroelastic properties	67
3.12	Hand lay-up process for composite fabrication	68
3.13	Sample for testing with pasted strain gauge at centre and emery cloth at sides	70
3.14	Thermal camera measuring SMA wire temperature	70
3.15	(a) Experimental setup for the tensile test of samples (b) Schematic diagram for the tensile test	72
3.16	Impact hammer modal test and signal processing	73

3.17	Marked samples for modal analysis (a) SMA wire at mid (b) SMA wire at near to trailing edge (c) SMA wire at near to leading edge	75
3.18	Experimental setup for impact hammer modal testing	76
3.19	3D woven composite sample mounted at base of wind tunnel at 0° angle of attack (a) Front view (b) Side view	78
3.20	Test sample with pasted triaxial strain gauge	79
3.21	Data acquisition setup for strain measurement	80
3.22	Digital manometer and pitot tube	81
3.23	Wind tunnel airspeed calibration test results	82
3.24	Wind tunnel flutter test set-up	83
3.25	(a) SMA-induced in-plane stresses in the composite plate without airflow (b) Uniform varying load applied by wind tunnel airflow to the composite plate (c) SMA-induced stresses in the composite plate under wind tunnel airflow	85
4.1	Resultant forces in the force-temperature curve	90
4.2	The load-Displacement curve of 2D plain woven laminated composites	91
4.3	Stress-strain graph of 2D plain woven laminated composites	91
4.4	Load-displacement curve of 3D orthogonal L2L interlock structures	93
4.5	Stress-strain graph of 3D orthogonal L2L interlock structures	93
4.6	Forces applied on fibres during tensile testing	94
4.7	Load-Displacement curve of 3D orthogonal TT interlock structures	95
4.8	Stress-strain graph of 3D orthogonal TT interlock structures	95

4.9	The load-displacement curve of 3D orthogonal modified interlock structures	97
4.10	Stress-strain graph of 3D orthogonal modified interlock structures	97
4.11	Comparison between the stiffness of 2D laminated and 3D composite structures without SMA wire, inactive and activated SMA wire	99
4.12	Comparison of the tensile strength of 2D laminated and 3D composite structures without SMA wire, inactive and activated SMA wire	101
4.13	Inactive 3D composites after tensile testing	102
4.14	Activated 3D composites after tensile testing	103
4.15	(a) SEM analysis of inactive 2D laminated composite (b) SEM analysis of activated 2D laminated composite	103
4.16	(a) SEM analysis of inactive L2L composite (b) SEM analysis of activated L2L composite	104
4.17	(a) SEM analysis of activated TT composite (b) SEM analysis of activated MF composite	105
4.18	FRF plot of impact hammer testing of aluminium plate	106
4.19	Comparison of natural frequencies of L2L without SMA wire, inactive and activated SMA wire at (a) Mid (b) Near to trailing edge (c) Near to leading edge	111
4.20	Comparison of natural frequencies of TT without SMA wire, inactive and activated SMA wire at (a) Mid (b) Near to trailing edge (c) Near to leading edge	113
4.21	Comparison of natural frequencies of MF without SMA wire, inactive and activated SMA wire at (a) Mid (b) Near to trailing edge (c) Near to leading edge	115

4.22	Aeroelastic behavior of L2L (a) Without SMA (b) Inactive SMA at mid (c) Activated SMA at mid (d) Inactive SMA at near to trailing edge (e) Activated SMA at near to trailing edge (f) Inactive SMA at near to leading edge (g) Activated SMA at near to leading edge	118
4.23	Flutter onset of L2L (a) Without SMA (b) Inactive SMA at mid (c) Activated SMA at mid (d) Inactive SMA at near to trailing edge (e) Activated SMA at near to trailing edge (f) Inactive SMA at near to leading edge (g) Activated SMA at near to leading edge	121
4.24	Aeroelastic behavior of TT (a) Without SMA (b) Inactive SMA at mid (c) Activated SMA at mid (d) Inactive SMA at near to trailing edge (e) Activated SMA at near to trailing edge (f) Inactive SMA at near to leading edge (g) Activated SMA at near to leading edge	124
4.25	Flutter onset of TT (a) Without SMA (b) Inactive SMA at mid (c) Activated SMA at mid (d) Inactive SMA at near to trailing edge (e) Activated SMA at near to trailing edge (f) Inactive SMA at near to leading edge (g) Activated SMA at near to leading edge	126
4.26	Aeroelastic behavior of MF (a) Without SMA (b) Inactive SMA at mid (c) Activated SMA at mid (d) Inactive SMA at near to trailing edge (e) Activated SMA at near to trailing edge (f) Inactive SMA at near to leading edge (g) Activated SMA at near to leading edge	128
4.27	Flutter onset of MF (a) Without SMA (b) Inactive SMA at mid (c) Activated SMA at mid (d) Inactive SMA at near to trailing edge (e) Activated SMA at near to trailing edge (f) Inactive SMA at near to leading edge (g) Activated SMA at near to leading edge	130
4.28	(a) Percentage reduction in flutter speed by activating SMA wire (b) Percentage reduction in flutter frequency by activating SMA wire	132
4.29	Percentage reduction in LCO amplitude of (a) Bending (b) Twist	132

LIST OF ABBREVIATIONS

AFFDL	Air Force Flight Dynamics Laboratory
ASTM	American Society of Testing and Materials
CNT	Carbon Nanotube
CPT	Classical Plate Theory
DAQ	Data Acquisition
DARPA	Defense Advanced Research Projects Agency
DSC	Differential Scanning Calorimetry
FEA	Finite Element Analysis
FG-CNTRC	Functionally Graded Carbon Nanotube Reinforced
FLIR	Forward-Looking Infrared
FRF	Frequency Response Function
FSDT	First-order Shear Deformation Plate Theory
GE	General Electric
GFRP	Glass Fibre Reinforced Polymer
GVT	Ground vibration testing
Hz	Hertz
LEAP	Leading Edge Aviation Propulsion
LCDs	Liquid Crystal Displays
LCO	Limit Cycle Oscillation
L2L	Layer-to-Layer
MF	Modified
MTS	Material Test System
NI	National Instruments
PDMS	Polydimethylsiloxane

RPM	Revolutions Per Minute
SEM	Scanning Electron Microscopy
SMA	Shape Memory Alloys
SME	Shape Memory Effect
SMAHC	Shape Memory Alloy Hybrid Composite
TT	Through-the-Thickness
UAV	Unmanned Aerial Vehicle
VARI	Vacuum-Assisted Resin Injection
VAT	Variable Angle Tow
2D	Two-Dimensional
3D	Three-Dimensional

CHAPTER 1

INTRODUCTION

1.1 Introduction

In aerospace, the study of interactions of airflow with aircraft is very important as this interaction can cause undesirable deformations and structural failures. This study is known as aeroelasticity and classified in static and dynamic aeroelasticity (Ashley, 1970). Structural divergence and flutter are the failure processes that are strongly affected by structural stiffness. The main area of interest is the flutter phenomenon that is a dynamic instability of elastic structure and it is a synchronized interaction between bending mode and twisting mode so that energy is absorbed from the airflow in one mode to increase the amplitude of the other. The wing will absorb energy from the airflow and will act as an increasing bending and torsion flexure until sufficient displacement is achieved and the wing breaks (Donadon & De Faria, 2016). In aircraft, metallic structures are mostly replaced by the composite structures due to their high stiffness and lighter weights (Dutton et al., 2004).

In composite structures, two-dimensional (2D) laminated composites have been used with outstanding success for many years in the aircraft industry (Mouritz et al., 1999; Kalanchiam & Chinnasamy, 2012). Despite the use of 2D laminates over a long period, their use in many structural applications has been limited due to their low through-the-thickness mechanical properties and inferior impact damage resistance as compared to aluminum alloys and steel (Mouritz et al., 1999). The low through-the-thickness properties have limited the use of 2D laminates to the structures, those are subjected to high through-the-thickness and interlaminar shear stresses such as automobiles, wind turbine blades, stringers and stiffeners in aircraft, and pressure vessels. In aeronautic under high vibrations, the delamination of plies occurs for laminated structures that results in structural failure and even more worst results for curved and angled pieces (Umair et al., 2015).

To improve through-the-thickness properties and interlayer fracture resistance, 3D woven interlock structures are used as composite reinforcement (Mishra, 2008; Nawab et al., 2012). 3D woven reinforcements have higher mechanical properties through-the-thickness direction and are used in areas of high-performance applications (Huang et al., 2018). In 3D woven structures, binder yarns travel in through-the-thickness direction to bind the layers with each other and are responsible for higher through-the-thickness properties, higher delamination resistance, and excellent damage tolerance (Mouritz et al., 1999; Khokar, 2001; Lee et al., 2002). Also for 3D structures, the desired properties can be incorporated during the weaving process and these structures can be produced according to the required shape (Soden & Hill, 1998).

Recently, the development of composite materials took advantage of their inherent heterogeneity and anisotropy to combine the traditional load-bearing functions of composite materials with novel functionalities in the form of embedded elements. By combining smart materials with composites, the properties of the resultant smart composites can be modified due to integrating functions of smart materials directly into the structures (Cohades & Michaud, 2018). Among smart materials, shape memory alloys (SMAs) are able to generate a relatively large deformation and then recover their deformed shape upon heating (Liang & Rogers, 1997). At low temperature, SMA actuators are plastically deformed by bending, stretching, compressing and twisting, and they return to their original shape and size by increasing temperature due to internal phase transformation process. This shape reformation process generates a thermal–mechanical driving force (Kim et al., 2011). This shape recovery property of SMA makes it the most suitable smart material for active control of the structures.

SMAs have two phases; the austenite phase having higher Young's modulus due to well-packed crystalline structures at a higher temperature and the martensite phase in which SMAs have loosely packed crystalline structures at a lower temperature and behave as elastomers. In the martensite phase when a load is applied to SMA, it accommodates the strain as its crystal planes unfold the lattice and begin to reorient with the direction of loading. This reorientation of the lattice is known as "detwinning" and it gives higher values of stiffness (Sharifishourabi et al., 2014). SMAs change their phase from martensite to austenite at a higher temperature and recover their residual deformation due to well-packed crystalline arrangement in the austenite phase (Lei et al., 2013). The coupling effect of SMAs in response to temperature and load signifies their importance and encourages their embedment in composite structures for improving structural properties.

Generally, pre-strained SMA wires are embedded into composite structures and the electric current is applied to activate the SMA wires. Due to electric current, resistance heat is generated in the SMA and a large additional internal force would then be induced accordingly into the structures (Kim et al., 2011). This induced internal force in SMA is responsible for improving the bending and torsional stiffness of the SMA embedded composite structures. Improved bending and torsional properties improve the dynamic and aeroelastic characteristics of the structures. Many researches has been carried out for improving dynamic and aeroelastic characteristics of the structures by embedding SMA wires in composites (Barzegari et al., 2012; Samadpour et al., 2016; Donadon & De Faria, 2016; Cao et al., 2017; Lin et al., 2020). These researches are limited to embedding SMA wires in 2D structures and mostly studies are computational work. 2D laminated composites are poor in through-the-thickness mechanical properties and SMA-induced stresses and temperature can cause delamination of plies that ultimately results in structural failures under high vibrations.

In this research, SMA wires are embedded into 3D woven structures for achieving improved mechanical properties due to SMA-induced force and higher through-the-thickness properties due to 3D structure. Further, the dynamics and aeroelastic properties are assessed for 3D woven composite configurations with SMA embedded at different positions to evaluate the effect of SMA and its positioning on the dynamic and aeroelastic performance of the structures.

1.2 Problem Statement

The laminated composites have replaced most of the metallic structures in aircraft due to their light-weight and high strength. During the flight, the aircraft undergoes the aeroelastic effects that can cause structural failure if the stiffness of the structures is not adequate. For achieving higher stiffness, the fibres with higher Young's modulus such as carbon fibres are used as a reinforcement of composite structures. The increment of high-performance fibres for improving stiffness results in brittleness and also increases the cost.

Although the laminated composites reinforced with high-performance fibres have higher in-plane mechanical properties but their through-the-thickness properties are poor and also these structures face delamination of plies when subjected to high vibrations that result in failures of structures (Nawab et al., 2018).

On the other hand, the 3D composites have higher through-the-thickness properties and delamination resistance but their in-plan properties are compromised due to the higher crimps in yarns (Stig & Hallström, 2013). While to prevent aeroelastic effects, the in-plane properties especially the stiffness of the structures should be higher.

SMA's are the smart materials embedded in structures for improving stiffness by activating wires. For embedding SMA wires in laminated composites, additional processes are required for improving interfacial strength between SMA wire and matrix for achieving desired properties (Yang et al., 2018).

Additionally, recent progress works on aeroelastic tailoring using smart materials are explored only for 2D laminated composites. Especially for SMA, most works reported are numerical findings due to the experimental challenges of embedding SMA's into a composite system. These computational studies are related to embedding SMA in resin and fibres and there is no research to date that explains the aeroelastic behavior of SMA-fibre woven composites (Barzegari et al., 2012; Samadpour et al., 2016; Donadon & De Faria, 2016; Cao et al., 2017; Lin et al., 2020).

So, there is a need to develop a smart composite structure for aircraft wing which has higher in-plane as well as through-the-thickness properties with a resistance to delamination and then experimental evaluation of its dynamic and aeroelastic flutter performance.

1.3 Research Objectives

This research has the main objective to improve the mechanical properties of 3D woven composites by embedding SMA wires and evaluate their dynamic and aeroelastic properties. The specific objectives are as follows:

1. To investigate and compare the tensile properties of 2D and 3D woven composite configurations without SMA wire, with inactive and activated SMA wire.
2. To assess the dynamic characteristics of 3D woven composite configurations without SMA wire, with inactive and activated SMA wire at mid, trailing and leading edge.
3. To evaluate the aeroelastic performance of 3D woven composite configurations without SMA wire, with inactive and activated SMA wire at mid, trailing and leading edge.

1.4 Scope of Research

This research is a fundamental structural study to modify the properties of glass-fibre reinforced 3D woven composite by embedding SMA wires. The basic purpose of the study is to improve the mechanical properties of the composite plate by using the stress generation property of SMA wires embedded in 3D woven structure and assess the dynamic and aeroelastic properties of SMA embedded 3D woven composites with improved mechanical properties.

This study is limited to the multi-layer 3D orthogonal interlock with layer-to-layer and through-the-thickness penetration of binding yarns due to the higher bending and shear rigidity of 3D orthogonal structures. The SMA wire is embedded span-wise in the composite plate with a lower volume fraction i.e. 0.389%. The span-wise direction of SMA contributes evenly to improve stiffness of whole structure and the lower volume fraction of SMA minimizes the effects of SMA activation temperature on matrix and fibres. On the other hand, to achieve higher effects of SMA-induced stresses on mechanical, modal and aeroelastic properties, the plate is designed a flexible structure with thickness of 0.7 mm. To keep same volume fraction of SMA wire for the samples of aeroelastic flutter test with tensile test samples, the calculated aspect ratio was 6. Also aspect ratio 6 gives the highly flexible structure whose flutter can be easily manifested under low airspeed.

As the current study is the fundamental experimental research to explore the aeroelastic flutter properties of SMA embedded 3D woven composite plate, the aeroelastic flutter properties are evaluated in subsonic laminar flow of open-circuit wind tunnel with Mach number, $M \sim 0.02$ and Reynolds number 1.2×10^5 . The lower Mach number and Reynolds numbers gives the smooth flow in which flutter performance of highly flexible plate can be precisely observed.

1.5 Thesis Layout

The thesis has five chapters in which Chapter 1 gives a brief introduction, objectives and the scope of the current study. Chapter 2 highlights the previous studies related to aeroelasticity and its types followed by a discussion on composites structures and smart materials. The studies related to composite passive tailoring for improving the aeroelastic performance are then presented and finally a discussion on embedding shape memory alloys for active tailoring of composites for improving aeroelastic performance. Chapter 3 is the methodology that described the materials, 3D weaving procedure of SMA embedded 3D structures and their composite fabrication method, testing methods for tensile, dynamic, and wind tunnel tests. Chapter 4 presents the results and discussion for the tensile, dynamic, and aeroelastic properties of SMA embedded 3D woven composites. Chapter 5 addresses the conclusion and recommendations for the future work.

REFERENCES

- Ahmad, K., & Rahman, H. (2013). Aeroelastic analysis of high aspect ratio wing in subsonic flow. *Proceedings of 2013 10th International Bhurban Conference on Applied Sciences & Technology (IBCAST)*, 219–223.
- Ahn, S. K., Kasi, R. M., Kim, S. C., Sharma, N., & Zhou, Y. (2008). Stimuli-responsive polymer gels. *Soft Matter*, 4(6), 1151-1157.
- Amandolese, X., Michelin, S., & Choquel, M. (2013). Low speed flutter and limit cycle oscillations of a two-degree-of-freedom flat plate in a wind tunnel. *Journal of Fluids and Structures*, 43, 244-255.
- Ansar, M., Xinwei, W., & Chouwei, Z. (2011). Modeling strategies of 3D woven composites: A review. *Composite Structures*, 93(8), 1947-1963.
- Ashley H. (1970). AEROELASTICITY. *Applied Mechanics Reviews*, 23(2), 119–129.
- ASTM D3171. (2015). Standard Test Methods for Constituent Content of Composite Materials. *ASTM Book of Standards*.
- ASTM D 3039. (2008). Tensile Properties of Polymer Matrix. *Standard Test Method for Tensile Properties of Polymer Matrix Composite Materials*.
- ASTM D 792. (2012). ASTM D792 Standard Test Methods for Density and Specific Gravity (Relative Density) of Plastics. *Annual Book of ASTM Standards*.
- ASTM Int. (2009). Standard Test Method for Transformation Temperature of Nickel-Titanium Alloys by thermal analysis. *Annual Book of ASTM Standards*.
- Attaran, A., Abang Haji Abdul Majid, D. L., Basri, S., Rafie, A., & Abdullah, E. (2008). Structural optimization of an aeroelastically tailored composite flat plate made of woven fiberglass/epoxy. *Acta Mechanica*, 196, 161–173.
- Aurrekoetxea, J., Zurbitu, J., Ortiz De Mendibil, I., Agirregomezkorta, A., Sánchez-Soto, M., & Sarrionandia, M. (2011). Effect of superelastic shape memory alloy wires on the impact behavior of carbon fiber reinforced in situ polymerized poly(butylene terephthalate) composites. *Materials Letters*, 65(5), 863–865.
- Balta, J. A., Michaud, V. J., Parlinska, M., Gotthard, R., & Manson, J. A. E. (2000). Adaptive composite materials processing. *Proceedings of the European Conference on Macromolecular Physics, Structure Development upon Polymer Processing: Physical Aspects, Guimaraes, Portugal*, 24–28.

- Barbarino, S., Saavedra Flores, E. I., Ajaj, R. M., Dayyani, I., & Friswell, M. I. (2014). A review on shape memory alloys with applications to morphing aircraft. *Smart Materials and Structures*, 23(6), 63001.
- Barlow, J. B., Rae, W. H., & Pope, A. (1999). Low-speed wind tunnel testing. *John Wiley & Sons*.
- Barzegari, M. M., Dardel, M., Fathi, A., & Ghadimi, M. (2012). Aeroelastic characteristics of cantilever wing with embedded shape memory alloys. *Acta Astronautica*, 79, 189-202.
- Baz, A., Poh, S., Ro, J., & Gilheany, J. (1995). Control of the natural frequencies of nitinol-reinforced composite beams. *Journal of Sound and Vibration*, 185, 171–185.
- Behera, B. K., & Dash, B. P. (2015). Mechanical behavior of 3D woven composites. *Materials and Design*, 67, 261-271.
- Behera, B. K., & Mishra, R. (2008). 3-Dimensional weaving. *Indian Journal of Fibre and Textile Research*, 33(3), 274–287.
- Bhattacharya, S. S., & Koranne, M. (2012). Novel method of weaving three-dimensional shapes. *International Journal of Clothing Science and Technology*.
- Bisplinghoff, R. L., Ashley, H., & Goland, M. (1963). Principles of Aeroelasticity. *Journal of Applied Mechanics*.
- Bollas, D., Pappas, P., Parthenios, J., & Galiotis, C. (2007). Stress generation by shape memory alloy wires embedded in polymer composites. *Acta Materialia*, 55(16), 5489-5499.
- Boussu, F., Legrand, X., Nauman, S., & Binetruy, C. (2008). *Mouldability of angle interlock fabric*, 8-10.
- Brinson, L. C. (1993). One-dimensional constitutive behavior of shape memory alloys: Thermomechanical derivation with non-constant material functions and redefined martensite internal variable. *Journal of Intelligent Material Systems and Structures*, 4(2), 229-242.
- Brooks, T. R., Martins, J. R. R. A., & Kennedy, G. J. (2019). High-fidelity aerostructural optimization of tow-steered composite wings. *Journal of Fluids and Structures*, 88, 122-147.
- Bucht, A., Pagel, K., Eppler, C., & Kunze, H. (2013). Industrial Applications of Shape Memory Alloys Potentials and Limitations. *Innovative Small Drives and Micro-Motor Systems; 9. GMM/ETG Symposium*, 9, 1–6.
- Buehler, W. J., Gilfrich, J. V., & Wiley, R. C. (1963). Effect of Low-Temperature Phase Changes on the Mechanical Properties of Alloys near Composition TiNi. *Journal of Applied Physics*, 34(5), 1475–1477.

- Cao, D., Shao, C., Xu, Y., & Zhao, H. (2017). Aero-Elastic Flutter Characteristics of Laminated Composite Panel Embedded with Shape Memory Alloy Wires. *Journal of Harbin Institute of Technology (New Series)*, 5.
- Chen, X., Taylor, L. W., & Tsai, L. ju. (2011). An overview on fabrication of three-dimensional woven textile preforms for composites. *Textile Research Journal*, 81(9), 932–944.
- Chiu, C. H., & Cheng, C. C. (2003). Weaving Method of 3D Woven Preforms for Advanced Composite Materials. *Textile Research Journal*, 73(1), 37–41.
- Chopra, I. (2002). Review of state of art of smart structures and integrated systems. In *AIAA Journal*, 40(11), 2145-2187
- Christiansen, L. E., Lehn-Schiøler, T., Mosekilde, E., Gránásy, P., & Matsushita, H. (2002). Nonlinear characteristics of randomly excited transonic flutter, 58(4-6), 385-405
- Cohades, A., & Michaud, V. (2018). Shape memory alloys in fibre-reinforced polymer composites. *Advanced Industrial and Engineering Polymer Research*, 1(1), 66-81.
- Collar, A. R. (1978). The first fifty years of aeroelasticity. *Aerospace (Royal Aeronautical Society Journal)*, 5(2), 12–20.
- Craig Roy, J. (2000). Coupling of substructures for dynamic analyses-an overview. *41st Structures, Structural Dynamics, and Materials Conference and Exhibit*, 1573.
- Cui, Z. D., Man, H. C., & Yang, X. J. (2003). Characterization of the laser gas nitrided surface of NiTi shape memory alloy. *Applied Surface Science*, 208–209(1), 388–393.
- Daghash, S. M., & Ozbulut, O. E. (2016). Characterization of superelastic shape memory alloy fiber-reinforced polymer composites under tensile cyclic loading. *Jmade*, 111, 504–512.
- Dawood, M., El-Tahan, M. W., & Zheng, B. (2015). Bond behavior of superelastic shape memory alloys to carbon fiber reinforced polymer composites. *Composites Part B: Engineering*, 77, 238–247.
- De Baets, P. W. G., Battoo, R. S., & Mavris, D. N. (2000). Aeroelastic analysis of a composite wingbox with varying root flexibility. *Collection of Technical Papers - AIAA/ASME/ASCE/AHS/ASC Structures, Structural Dynamics and Materials Conference*.
- De Leon, D., de Souza, C., fonseca, jun, & Silva, R. (2010). Aeroelastic Tailoring of Composite Plates Through Eigenvalues Optimization. *Mecánica Computacional*, 29(7), 609-623.

- Dillinger, J. K. S., Klimmek, T., Abdalla, M. M., & Gürdal, Z. (2013). Stiffness optimization of composite wings with aeroelastic constraints. *Journal of Aircraft*, 50(4), 1159-1168.
- Donadon, M. V., & De Faria, A. R. (2016). Aeroelastic behavior of composite laminated shells with embedded SMA wires under supersonic flow. *Aerospace Science and Technology*, 52, 157–166.
- Dong, S., Katoh, Y., & Kohyama, A. (2003). Preparation of SiC/SiC composites by hot pressing, using tyranno-SA fiber as reinforcement. *Journal of the American Ceramic Society*, 86(1), 26–32.
- Dowell, e. H. (1975). *Aeroelasticity of plates and shells*, 1(1)
- Dym, C. L., & Shames, I. H. (1973). *Solid mechanics*. Springer.
- Dynalloy. (2020). *Flexinol® Actuator Wire Technical and Design Data*. https://www.dynalloy.com/tech_data_wire.php
- Earl, D., & Ye, W. (1991). Limit cycle oscillation of a fluttering cantilever plate. *AIAA Journal*, 29(11), 1929-1936.
- El-Dessouky, H. M., Snape, A. E., Turner, J. L., Saleh, M. N., Tew, H., & Scaife, R. J. (2017). 3D weaving for advanced composite manufacturing: from research to reality. *Proceedings of the SAMPE Conference*.
- Eriksson, S., Berglin, L., Gunnarsson, E., Guo, L., Lindholm, H., & Sandsjö, L. (2010). Three-dimensional multilayer fabric structures for interactive textiles. *Proceedings of the 3rd World Conference on 3D Fabrics and Their Applications*.
- Ewins, D. J. (2000). *Modal Testing: Theory, Practice and Application (Mechanical Engineering Research Studies: Engineering Dynamics Series)*. Research Studies Press Ltd.
- Formenti, D., & Richardson, M. (2002). Parameter Estimation from Frequency Response Measurements using Rational Fraction Polynomials (Twenty Years of Progress). *IMAC Conference*.
- Furuya, Y., & Shimada, H. (1991). Shape memory actuators for robotic applications. *Materials and Design*, 12(1), 21–28.
- Furuya, Yasubumi. (1996). Design and Material Evaluation of Shape Memory Composite. *Journal of Intelligent Material Systems and Structures*, 7(3), 321–330.
- Garafolo, N. G., & McHugh, G. R. (2018). Mitigation of flutter vibration using embedded shape memory alloys. *Journal of Fluids and Structures*, 76, 592-605.

- Garrick, I. E., & Reed, W. H. (1981). Historical development of aircraft flutter. *Journal of Aircraft*, 18(11), 897–912.
- Gibbs IV, S. C., Wang, I., & Dowell, E. H. (2015). Stability of rectangular plates in subsonic flow with various boundary conditions. *Journal of Aircraft*, 52(2), 439–451.
- Gibbs, S. C., Sethna, A., Wang, I., Tang, D., & Dowell, E. (2014). Aeroelastic stability of a cantilevered plate in yawed subsonic flow. *Journal of Fluids and Structures*, 49, 450–462.
- Göge, D., Böswald, M., Füllekrug, U., & Lubrina, P. (2007). Ground Vibration Testing of Large Aircraft -State-of-the-Art and Future Perspectives.
- Green, J. A. (1987). Aeroelastic tailoring of aft-swept high-aspect-ratio composite wings. *Journal of Aircraft*, 24(11), 812-819.
- Gu, B. (2016). Modelling of 3D woven fabrics for ballistic protection. *Advanced Fibrous Composite Materials for Ballistic Protection*, 145-197.
- Gu, H., & Zhili, Z. (2002). Tensile behavior of 3D woven composites by using different fabric structures. *Materials and Design*, 23(7), 671–674.
- Gu, X., Su, X., Wang, J., Xu, Y., Zhu, J., & Zhang, W. (2020). Improvement of impact resistance of plain-woven composite by embedding superelastic shape memory alloy wires. *Frontiers of Mechanical Engineering*, 1–11.
- Guo, S. J., Bannerjee, J. R., & Cheung, C. W. (2003). The effect of laminate lay-up on the flutter speed of composite wings. *Proceedings of the Institution of Mechanical Engineers, Part G: Journal of Aerospace Engineering*, 217(3), 115-122.
- Guo, S., Li, D., & Liu, Y. (2012). Multi-objective optimization of a composite wing subject to strength and aeroelastic constraints. *Proceedings of the Institution of Mechanical Engineers, Part G: Journal of Aerospace Engineering*, 226(9), 1095-1106.
- Guo, X., Lee, Y. Y., & Mei, C. (2007). Supersonic nonlinear panel flutter suppression using shape memory alloys. *Journal of Aircraft*, 44(4), 1139-1149.
- Haidzir, H., Majid, D. L., Rafie, A. S. M., & Harmin, M. Y. (2014). Modal properties of hybrid carbon/kevlar composite thin plate and hollow wing model. *Applied Mechanics and Materials*, 446, 597-601.
- Han, M. W., Rodrigue, H., Cho, S., Song, S. H., Wang, W., Chu, W. S., & Ahn, S. H. (2016). Woven type smart soft composite for soft morphing car spoiler. *Composites Part B: Engineering*, 86, 285–298.

- Han, M. W., Rodrigue, H., Kim, H. II, Song, S. H., & Ahn, S. H. (2016). Shape memory alloy/glass fiber woven composite for soft morphing winglets of unmanned aerial vehicles. *Composite Structures*, 140, 202–212.
- Haresceugh, R. I., Bowen, D. H., Bonfield, W., Hodgson, A. A., Gent, A. N., Livingston, D. I., & Beardmore, P. (1994). Aircraft and Aerospace Applications of Composites. In *Concise Encyclopedia of Composite Materials*, 1–31.
- Hart, K. R., Chia, P. X. L., Sheridan, L. E., Wetzel, E. D., Sottos, N. R., & White, S. R. (2017). Comparison of Compression-After-Impact and Flexure-After-Impact protocols for 2D and 3D woven fiber-reinforced composites. *Composites Part A: Applied Science and Manufacturing*, 101, 471-479.
- Hartl, D. J., & Lagoudas, D. C. (2007). Aerospace applications of shape memory alloys. *Proceedings of the Institution of Mechanical Engineers, Part G: Journal of Aerospace Engineering*, 221(4), 535–552.
- Hibbeler, R. C. (2001). Mechanics of Materials Eighth Edition. In *Pearson Prentice Hall*.
- Hollowell, S. J., & Dugundji, J. (1984). Aeroelastic flutter and divergence of stiffness coupled, graphite/epoxy cantilevered plates. *Journal of Aircraft*, 21(1), 69–76.
- Hopkins, M., & Dowell, E. (1994). Limited amplitude panel flutter with a temperature differential. *35th Structures, Structural Dynamics, and Materials Conference*, 1486.
- Hornbogen, E. (1989). Shape memory alloys. *Practical Metallography*, 26(6), 279-294.
- Housner, J. M., & Stein, M. (1974). Flutter Analysis of Swept Wing Subsonic Aircraft With Parameter Studies of Composite Wings. *Technical Note*.
- Huang, T., Wang, Y., & Wang, G. (2018). Review of the Mechanical Properties of a 3D Woven Composite and Its Applications. *Polymer - Plastics Technology and Engineering*, 57(8), 740-756.
- Huang, W. (1998). Shape memory alloys and their application to actuators for deployable structures.
- Huang, W. M., Ding, Z., Wang, C. C., Wei, J., Zhao, Y., & Purnawali, H. (2010). Shape memory materials. *Materials Today*, 13(7-8), 54-61.
- Hurty, W. C. (1965). Dynamic analysis of structural systems using component modes. *AIAA Journal*, 3(4), 678-685.

- Hussein, A. M. H., Majid, D. L., & Abdullah, E. J. (2016). Shape memory alloy actuation effect on subsonic static aeroelastic deformation of composite cantilever plate. *MS&E*, 152(1), 12010.
- Ibrahim, H. H., Yoo, H. H., & Lee, K. S. (2009). Thermal buckling and flutter behavior of shape memory alloy hybrid composite shells. *Journal of Aircraft*, 46(3), 895-902.
- Inman, D. J. (2007). Smart Materials and Structures. In *CISM International Centre for Mechanical Sciences, Courses and Lectures*.
- Isogai, K. (1992). Transonic flutter/divergence characteristics of aeroelastically tailored and non-tailored high-aspect-ratio forward-swept wings. *Journal of Fluids and Structures*, 6(5), 525-537.
- Jamshidi, S., Dardel, M., & Pashaei, M. H. (2016). Investigating the effects of ionic polymer metal composite patches on aeroelastic characteristics of a cantilever wing in supersonic flow. *Scientia Iranica*, 23(2), 575-587.
- Jang, B. K., & Kishi, T. (2005). Adhesive strength between TiNi fibers embedded in CFRP composites. *Materials Letters*, 59(11), 1338–1341.
- Jani, M. J., Leary, M., Subic, A., & Gibson, M. A. (2014). A review of shape memory alloy research, applications and opportunities. *Materials and Design*, 56, 1078–1113.
- Jin, L., Niu, Z., Jin, B. C., Sun, B., & Gu, B. (2012). Comparisons of static bending and fatigue damage between 3D angle-interlock and 3D orthogonal woven composites. *Journal of Reinforced Plastics and Composites*, 31(14), 935–945.
- Ju, Q., & Qin, S. (2009). New Improved g Method for Flutter Solution. *Journal of Aircraft*, 46(6), 2184–2186.
- Jung, B.-S., Kim, M.-S., Kim, J.-S., Kim, Y.-M., Lee, W.-Y., & Ahn, S.-H. (2010). Fabrication of a smart air intake structure using shape memory alloy wire embedded composite. *Physica Scripta*, 2010(T139), 014042.
- Jung, B. S., Kim, M. S., Kim, Y. M., & Ahn, S. H. (2010). Fabrication of smart structure using shape memory alloy wire embedded hybrid composite. *Materialwissenschaft Und Werkstofftechnik*, 41(5), 320–324.
- Jutte, C., & Stanford, B. K. (2014). Aeroelastic Tailoring of Transport Aircraft Wings: State-of-the-Art and Potential Enabling Technologies. *Nasa*, April, 34.
- Kalanchiam, M., & Chinnasamy, M. (2012). Advantages of composite materials in aircraft structures. *World Academy of Science, Engineering and Technology*, 71(11), 597–601.

- Kameyama, M., & Fukunaga, H. (2007). Optimum design of composite plate wings for aeroelastic characteristics using lamination parameters. *Computers and Structures*, 85(3-4), 213-224.
- Kang, K. W., & Kim, J. K. (2009). Effect of shape memory alloy on impact damage behavior and residual properties of glass/epoxy laminates under low temperature. *Composite Structures*, 88(3), 455–460.
- Kauffman, G. B., & MAYO, I. (1997). The Story of Nitinol: The Serendipitous Discovery of the Memory Metal and Its Applications. *The Chemical Educator*, 2(2), 1–21.
- Kenway, G. K. W., Kennedy, G. J., & Martins, J. R. R. A. (2014). Scalable parallel approach for high-fidelity steady-state aeroelastic analysis and adjoint derivative computations. *AIAA Journal*, 52(5), 935–951.
- Khan, M. I., Mukherjee, K., Shoukat, R., & Dong, H. (2017). A review on pH sensitive materials for sensors and detection methods. *Microsystem Technologies*, 23(10), 4391-4404.
- Khokar, N. (2001). 3D-Weaving: Theory and Practice. *Journal of the Textile Institute*, 92(2), 193-207.
- Kim, B. C., Hazra, K., Weaver, P., & Potter, K. (2011). Limitations of fibre placement techniques for variable angle tow composites and their process-induced defects. *ICCM International Conferences on Composite Materials*, 21-26.
- Kim, E. H., Lee, I., Roh, J. H., Bae, J. S., Choi, I. H., & Koo, K. N. (2011). Effects of shape memory alloys on low velocity impact characteristics of composite plate. *Composite Structures*, 93(11), 2903–2909.
- Koo, K. N., & Lee, I. (1994). Aeroelastic behavior of a composite plate wing with structural damping. *Computers and Structures*, 50(2), 167-176.
- Krenkel, W., & Berndt, F. (2005). C/C–SiC composites for space applications and advanced friction systems. *Materials Science and Engineering: A*, 412(1), 177–181.
- Krone, Jr., N. (1975). Divergence elimination with advanced composites. *Aircraft Systems and Technology Meeting*, 1009.
- Kuo, S. Y., Shiau, L. C., & Chen, K. H. (2009). Buckling analysis of shape memory alloy reinforced composite laminates. *Composite Structures*, 90(2), 188–195.
- Kuo, S. Y., Shiau, L. C., & Lai, C. H. (2012). Flutter of buckled shape memory alloy reinforced laminates. *Smart Materials and Structures*, 21(3), 035020.
- Lampert, C. M. (2004). Chromogenic smart materials. *Materials Today*, 7(3), 28-35.

- Lanchester, F. W. (1916). Torsional Vibrations of the Tail of an Aeroplane. *Aeronaut. Research Com. R & M*, 276.
- Larco, C., Pahonie, R., & Edu, I. (2015). The effects of fibre volume fraction on a glass-epoxy composite material. *Incas Bulletin*, 7(3), 113.
- Lau, K. T., Zhou, L. M., & Tao, X. M. (2002). Control of natural frequencies of a clamped-clamped composite beam with embedded shape memory alloy wires. *Composite Structures*, 58(1).
- Lee, I.-W., Kim, D.-O., & Jung, G.-H. (1999). Natural frequency and mode shape sensitivities of damped systems: part I, distinct natural frequencies. *Journal of Sound and Vibration*, 223(3), 399–412.
- Lee, L., Rudov-Clark, S., Mouritz, A. P., Bannister, M. K., & Herszberg, I. (2002). Effect of weaving damage on the tensile properties of three-dimensional woven composites. *Composite Structures*, 57(1-4), 405-413.
- Lei, H., Wang, Z., Tong, L., Zhou, B., & Fu, J. (2013). Experimental and numerical investigation on the macroscopic mechanical behavior of shape memory alloy hybrid composite with weak interface. *Composite Structures*, 101, 301–312.
- Lexcellent, C., Leclercq, S., Gabry, B., & Bourbon, G. (2000). Two way shape memory effect of shape memory alloys: an experimental study and a phenomenological model. *International Journal of Plasticity*, 16(10-11), 1155-1168.
- Li, J., & Y.B, J. (2012). Application and Development of Composite Materials for GE New Generation Civil Aero- Engine. *The 17th National Conference on Composite Materials, China*.
- Li, P., Yang, Y., & Xu, W. (2012). Nonlinear dynamics analysis of a two-dimensional thin panel with an external forcing in incompressible subsonic flow. *Nonlinear Dynamics*, 67(4), 2483–2503.
- Li, P., Yang, Y., Xu, W., & Chen, G. (2012). On the aeroelastic stability and bifurcation structure of subsonic nonlinear thin panels subjected to external excitation. *Archive of Applied Mechanics*, 82(9), 1251–1267.
- Liang, C., & Rogers, C. A. (1997). Design of shape memory alloy actuators. *Journal of Intelligent Material Systems and Structures*, 8(4), 303–313.
- Lin, H., Shao, C., & Cao, D. (2020). Nonlinear flutter and random response of composite panel embedded in shape memory alloy in thermal-aero-acoustic coupled field. *Aerospace Science and Technology*, 100, 105785.
- Lin, K.-J., Lu, P.-J., & Tarn, J.-Q. (1989). Flutter analysis of cantilever composite plates in subsonic flow. *AIAA Journal*, 27(8), 1102–1109.

- Liu, Y., Wang, Z., Li, H., Sun, M., Wang, F., & Chen, B. (2018). Influence of Embedding SMA Fibres and SMA Fibre Surface Modification on the Mechanical Performance of BFRP Composite Laminates. *Materials*, 11, 70.
- Long, A. C. (2005). Design and manufacture of textile composites. *Design and Manufacture of Textile Composites*.
- Lu, S. F., Jiang, Y., Zhang, W., & Song, X. J. (2020). Vibration suppression of cantilevered piezoelectric laminated composite rectangular plate subjected to aerodynamic force in hygrothermal environment. *European Journal of Mechanics-A/Solids*, 83, 104002.
- Lubin, G., & Klerer, J. (1970). Handbook of Fiberglass and Advanced Plastics Composites. *Journal of The Electrochemical Society*, 117(7), 219C.
- Ma, L., Yao, M., Zhang, W., Lou, K., Cao, D., & Niu, Y. (2020). A Novel Aerodynamic Force and Flutter of the High-Aspect-Ratio Cantilever Plate in Subsonic Flow. *Shock and Vibration*, 2020.
- Majid, D. L. A. H. A., & Basri, S. (2008). LCO flutter of cantilevered woven glass/epoxy laminate in subsonic flow. *Acta Mechanica Sinica*, 24(1), 107–110.
- Mani, Y., & Senthilkumar, M. (2015). Shape memory alloy-based adaptive-passive dynamic vibration absorber for vibration control in piping applications. *Journal of Vibration and Control*, 21(9), 1838–1847.
- Manjunatha, G. R., Rajanna, K., Mahapatra, D. R., Nayak, M. M., Krishnaswamy, U. M., & Srinivasa, R. (2013). Polyvinylidene fluoride film based nasal sensor to monitor human respiration pattern: An initial clinical study. *Journal of Clinical Monitoring and Computing*, 27(6), 647–657.
- Mark, R., & Robinson, A. (1976). Principles of weaving. *The Textile institute*, p-249.
- Marsh, G. (2012). Aero engines lose weight thanks to composites. *Reinforced Plastics*, 56(6), 32-35.
- Marshall, J. A. (2002). Smart materials. *ASEE Annual Conference Proceedings*.
- McIntyre, J. E. (2004). Synthetic fibres: Nylon, polyester, acrylic, polyolefin. *Synthetic Fibres: Nylon, Polyester, Acrylic, Polyolefin*.
- Meddaikar, Y. M., Dillinger, J. K. S., Sodja, J., Mai, H., & de Breuker, R. (2015). Optimization, manufacturing and testing of a composite wing with maximized tip deflection. *57th AIAA/ASCE/AHS/ASC Structures, Structural Dynamics, and Materials Conference*.

- Mei, C. (1977). A finite-element approach for nonlinear panel flutter. *AIAA Journal*, 15(8), 1107–1110.
- Meo, M., Marulo, F., Guida, M., & Russo, S. (2013). Shape memory alloy hybrid composites for improved impact properties for aeronautical applications. *Composite Structures*, 95, 756–766.
- Miková, L., Medvecká, S., Kelemen, B. M., Trebuňa, F., & Virgala, I. (2015). Application of Shape Memory Alloy (SMA) as Actuator. *Metalurgija*, 54(1), 169–172.
- Mishra, R. (2008). 3-Dimensional weaving. 33, 274–287.
- Mouritz, A. P., Bannister, M. K., Falzon, P. J., & Leong, K. H. (1999). Review of applications for advanced three-dimensional fibre textile composites. *Composites Part A: Applied Science and Manufacturing*, 30(12), 1445–1461.
- Murkute, V., Gupta, A., Thakur, D. G., Harshe, R., & Joshi, M. (2014). Improvisation of Interfacial Bond Strength in Shape Memory Alloy Hybrid Polymer Matrix Composites. *Procedia Materials Science*, 6(Icmpc), 316–321.
- Nader, G., dos Santos, C., Jabardo, P. J. S., Cardoso, M., Taira, N. M., & Pereira, M. T. (2006). Characterization of low turbulence wind tunnel. *XVIII IMEKO World Congress, Rio de Janeiro, Brazil, September*.
- Nahom Jidovetski, T., Raveh, D. E., & Iovnovich, M. (2019). Wind-Tunnel Study of the Autoregressive Moving-Average Flutter Prediction Method. *Journal of Aircraft*, 56(4), 1441–1454.
- Nawab, Y., Legrand, X., & Koncar, V. (2012). Study of changes in 3D-woven multilayer interlock fabric preforms while forming. *Journal of the Textile Institute*, 103(12), 1273–1279.
- Nawab, Y., Kashif, M., Asghar, M. A., Umair, M., Shaker, K., & Zeeshan, M. (2018). Development & characterization of green composites using novel 3D woven preforms. *Applied Composite Materials*, 25(4), 747–759.
- Nayak, N. V. (2014). Composite Materials in Aerospace Applications. *International Journal of Scientific and Research Publications*, 4(9), 1-10.
- Ni, Q. Q., Zhang, R. x., Natsuki, T., & Iwamoto, M. (2007). Stiffness and vibration characteristics of SMA/ER3 composites with shape memory alloy short fibers. *Composite Structures*, 79(4), 501–507.
- Olander, A. (1932). An Electrochemical Investigation Of Solid Cadmium-Gold Alloys. *Journal of the American Chemical Society*, 54(10), 3819–3833.
- Packard, H. (1997). The fundamentals of modal testing. *Methods*.

- Pappadà, S., Rametta, R., Toia, L., Coda, A., Fumagalli, L., & Maffezzoli, A. (2009). Embedding of superelastic SMA wires into composite structures: Evaluation of impact properties. *Journal of Materials Engineering and Performance*, 18(5–6), 522–530.
- Park, J. S., Kim, J. H., & Moon, S. H. (2005). Thermal post-buckling and flutter characteristics of composite plates embedded with shape memory alloy fibers. *Composites Part B: Engineering*, 36(8).
- Parthiban, R., & Senthil Kumaran, S. (2015). Vibration analysis of composite material in thermal environmental. *International Journal of Applied Engineering Research*, 10(9), 534-539.
- Patil, M. J., Hodges, D. H., & Cesnik, C. E. S. (2001). Limit-cycle oscillations in high-aspect-ratio wings. *Journal of Fluids and Structures*, 15(1), 107–132.
- Pequegnat, A., Michael, A., Wang, J., Lian, K., Zhou, Y., & Khan, M. I. (2015). Surface characterizations of laser modified biomedical grade NiTi shape memory alloys. *Materials Science and Engineering C*, 50, 367–378.
- Petrini, L., & Migliavacca, F. (2011). Biomedical Applications of Shape Memory Alloys. *Journal of Metallurgy*, 1–15.
- Qin, L., Zhang, Z., Li, X., Yang, X., Feng, Z., Wang, Y., Miao, H., He, L., & Gong, X. (2012). Full-field analysis of shear test on 3D orthogonal woven C/C composites. *Composites Part A: Applied Science and Manufacturing*, 43(2), 310-316.
- Quilter, A. (2004). Composites in Aerospace Applications. *Information Handling Services, Inc. (IHS)*.
- Raghavan, J., Bartkiewicz, T., Boyko, S., Kupriyanov, M., Rajapakse, N., & Yu, B. (2010). Damping, tensile, and impact properties of superelastic shape memory alloy (SMA) fiber-reinforced polymer composites. *Composites Part B: Engineering*, 41(3), 214–222.
- Raveh, D. E. (2004). Identification of computational-fluid-dynamics based unsteady aerodynamic models for aeroelastic analysis. *Journal of Aircraft*, 41(3), 620–632.
- Rudov-Clark, S. and, & Mouritz, A. P. (2008). Tensile fatigue properties of a 3D orthogonal woven composite. *Composites Part A: Applied Science and Manufacturing*, 39(6), 1018–1024.
- Saleh, M. N., & Soutis, C. (2017). Recent advancements in mechanical characterisation of 3D woven composites. *Mechanics of Advanced Materials and Modern Processes*, 3(1).

- Saleh, M. N., Yudhanto, A., Potluri, P., Lubineau, G., & Soutis, C. (2016). Characterising the loading direction sensitivity of 3D woven composites: Effect of z-binder architecture. *Composites Part A: Applied Science and Manufacturing*, 90, 577-588.
- Samadpour, M., Asadi, H., & Wang, Q. (2016). Nonlinear aero-thermal flutter postponement of supersonic laminated composite beams with shape memory alloys. *European Journal of Mechanics, A/Solids*, 57, 18-28.
- Sawant, S. U., Chauhan, S. J., & Deshmukh, N. N. (2017). Effect of crack on natural frequency for beam type of structures. *AIP Conference Proceedings*, p-020056.
- Schoeppner, G. A., & Abrate, S. (2000). Delamination threshold loads for low velocity impact on composite laminates. *Composites Part A: Applied Science and Manufacturing*, 31(9), 903–915.
- Schrooten, J., Michaud, V., & Parthenios, J. (2002). Progress on composites with embedded shape memory alloy wires. *Materials Transactions*, 43(5), 961–973.
- Sharifishourabi, G., Alebrahim, R., Sharifi, S., Ayob, A., Vrcelj, Z., & Yahya, M. Y. (2014). *Mechanical Properties of potentially Smart Carbon Epoxy Composites with Asymmetrically Embedded Shape Memory Wires*. 59, 486–493.
- Sherrer, V. C., Hertz, T. J., & Shirk, M. H. (1981). Wind tunnel demonstration of aeroelastic tailoring applied to forward swept wings. *Journal of Aircraft*, 18(11).
- Shirk, M. H., Hertz, T. J., & Weisshaar, T. A. (1986). Aeroelastic Tailoring - Theory, Practice, and Promise. *Journal of Aircraft*, 23(1), 6–18.
- Shoel, K., & Mittal, R. (2016). Flutter instability of a thin flexible plate in a channel. *Journal of Fluid Mechanics*, 786, 29.
- Shyr, T. W., & Pan, Y. H. (2003). Impact resistance and damage characteristics of composite laminates. *Composite Structures*, 62(2), 193–203.
- Smilg, B. (1949). The Instability of Pitching Oscillations of an Airfoil in Subsonic Incompressible Potential Flow. *Journal of the Aeronautical Sciences*, 16(11), 691-696.
- Smith, N. A., Antoun, G. G., Ellis, A. B., & Crone, W. C. (2004). Improved adhesion between nickel-titanium shape memory alloy and a polymer matrix via silane coupling agents. *Composites Part A: Applied Science and Manufacturing*, 35(11), 1307–1312.
- Smooth-On. (2020). *EpoxAmite™ 100 Epoxy Laminating System*. https://www.smooth-on.com/tb/files/Epoxamite_TB.

- Soden, J. A., & Hill, B. J. (1998). Conventional weaving of shaped preforms for engineering composites. *Composites Part A: Applied Science and Manufacturing*, 29(7), 757-762.
- Sriram, A. T., & Narahari, H. K. (2020). Study of Wing Flutter at Preliminary Stages of Design. *Advances in Multidisciplinary Analysis and Optimization*, 77–84.
- Stanford, B. K., Jutte, C. V., & Chauncey Wu, K. (2014). Aeroelastic benefits of tow steering for composite plates. *Composite Structures*, 118, 416-422.
- Stig, F., & Hallström, S. (2013). Influence of crimp on 3D-woven fibre reinforced composites. *Composite Structures*, 95, 114-122.
- Stodieck, O., Cooper, J. E., Weaver, P. M., & Kealy, P. (2017). Aeroelastic tailoring of a representative wing box using tow-steered composites. *AIAA Journal*, 55(4), 1425-1439.
- Stodieck, Olivia, Cooper, J. E., Weaver, P. M., & Kealy, P. (2013). Improved aeroelastic tailoring using tow-steered composites. *Composite Structures*, 106, 703-715.
- Stoeckel, D. (1991). Shape Memory Actuators for Automotive. *MATERIALS & DESIGN*, 11(6), 302–307.
- Sujan, D., Oo, Z., Rahman, M. E., Maleque, M. A., & Tan, C. K. (2012). Physio-mechanical properties of Aluminium metal matrix composites reinforced with Al₂O₃ and SiC. *International Journal of Materials and Metallurgical Engineering*, 6(8), 678–681.
- Sun, L., Huang, W. M., Ding, Z., Zhao, Y., Wang, C. C., Purnawali, H., & Tang, C. (2012). Stimulus-responsive shape memory materials: A review. *Materials and Design*, 33(1), 577–640.
- Sun, Z., Xu, Y., & Wang, W. (2019). Experimentation of the bilinear elastic behavior of plain-woven GFRP composite with embedded SMA wires. *Polymers*, 11(3), 405.
- Sunar, M. (2018). Piezoelectric Materials. *Comprehensive Energy Systems*.
- Swain, P. K., Adhikari, B., Maiti, D. K., & Singh, B. N. (2019). Aeroelastic analysis of CNT reinforced functionally graded laminated composite plates with damage under subsonic regime. *Composite Structures*, 222, 110916.
- Sylvester, M. A., & Baker, J. E. (1952). Some experimental studies of panel flutter at Mach number 1.3. *National Advisory Committee for Aeronautics*.
- Tang, D., & Dowell, E. H. (2002). Limit cycle oscillations of two-dimensional panels in low subsonic flow. *International Journal of Non-Linear Mechanics*, 37(7), 1199–1209.

- Tang, D., Dowell, E. H., & Hall, K. C. (1999). Limit Cycle Oscillations of a Cantilevered Wing in Low Subsonic Flow. *AIAA Journal*, 37(3), 364-371.
- Turner, P., Liu, T., & Zeng, X. (2016). Collapse of 3D orthogonal woven carbon fibre composites under in-plane tension/compression and out-of-plane bending. *Composite Structures*, 142, 286-297.
- Umair, M., Nawab, Y., Malik, M. H., & Shaker, K. (2015). Development and characterization of three-dimensional woven-shaped preforms and their associated composites. *Journal of Reinforced Plastics and Composites*, 34(24), 2018-2028.
- Umer, R., Alhusein, H., Zhou, J., & Cantwell, W. J. (2017). The mechanical properties of 3D woven composites. *Journal of Composite Materials*, 51(12), 1703-1716.
- Van Langenhove, L., & Hertleer, C. (2004). Smart clothing: a new life. *International Journal of Clothing Science and Technology*, 16(1/2), 63–72.
- Voß, A., & Ohme, P. (2018). Dynamic maneuver loads calculations for a sailplane and comparison with flight test. *CEAS Aeronautical Journal*, 9(3), 445–460.
- Wang, L., Shen, L., Chen, L., Wu, Z., & Yang, C. (2012). Design and analysis of a wind tunnel test model system for gust alleviation of aeroelastic aircraft. *Collection of Technical Papers - AIAA/ASME/ASCE/AHS/ASC Structures, Structural Dynamics and Materials Conference*.
- Wang, Z., Xu, L., Sun, X., Shi, M., & Liu, J. (2017). Fatigue behavior of glass-fiber-reinforced epoxy composites embedded with shape memory alloy wires. *Composite Structures*, 178, 311–319.
- Weisshaar, T. A. (1981). Aeroelastic tailoring of forward swept composite wings. *Journal of Aircraft*, 18(8), 669-676.
- Weisshaar, T., Nam, C., & Batista-Rodriguez, A. (1998). *Aeroelastic tailoring for improved UAV performance*, p-1757.
- Wu, R., Han, M. W., Lee, G. Y., & Ahn, S. H. (2013). Woven type smart soft composite beam with in-plane shape retention. *Smart Materials and Structures*, 22(12).
- Wu, Z., Raju, G., & Weaver, P. M. (2015). Framework for the buckling optimization of variable-angle tow composite plates. *AIAA Journal*, 53(12), 3788-3804.
- Yan, S., Zeng, X., & Long, A. (2018). Experimental assessment of the mechanical behaviour of 3D woven composite T-joints. *Composites Part B: Engineering*, 154, 108-113.

- Yang, B., Zhang, Y., Xuan, F.-Z., Xiao, B., He, L., & Gao, Y. (2018). Improved adhesion between nickel–titanium SMA and polymer matrix via acid treatment and nano-silica particles coating. *Advanced Composite Materials*, 27(3), 331–348.
- Yang, J., Faverjon, B., Peters, H., & Kessissoglou, N. (2014). Modal analysis and frequency response of a flexible plate with uncertain properties using polynomial chaos expansion. *21st International Congress on Sound and Vibration 2014, ICSV 2014*.
- Yang, S. M., Han, J. H., & Lee, I. (2006). Characteristics of smart composite wing with SMA actuators and optical fiber sensors. *International Journal of Applied Electromagnetics and Mechanics*, 23(3-4), 177-186.
- Yin, Q., Lardeur, P., & Druesne, F. (2018). Performances assessment of the Modal Stability Procedure for the probabilistic free vibration analysis of laminated composite structures. *Composite Structures*, 203, 474-485.
- Yoon, N. K., Chung, C. H., Na, Y. H., & Shin, S. J. (2012). Control reversal and torsional divergence analysis for a high-aspect-ratio wing. *Journal of Mechanical Science and Technology*, 26(12), 3921-3931.
- Yuniu(2018). *Yuniu Fiberglass Manufacturing*.
<https://www.fiberglassyn.com/Fiberglass-Roving-pl518235.html>
- Yuvaraja, M., & Senthilkumar, M. (2013). Comparative study on vibration characteristics of a flexible GFRP composite beam using SMA and PZT actuators. *Procedia Engineering*, 64, 571–581.
- Zai, B., Ahmad, F., Lee, C., Kim, T.-O., & Park, M. kyun. (2011). Structural Optimization of Cantilever Beam in Conjunction with Dynamic Analysis. *Journal of the Korean Institute of Gas*, 15, 31–36.
- Zhang, R. x., Ni, Q. Q., Natsuki, T., & Iwamoto, M. (2007). Mechanical properties of composites filled with SMA particles and short fibers. *Composite Structures*, 79(1), 90–96.
- Zhang, R. xin, Ni, Q. Q., Masuda, A., Yamamura, T., & Iwamoto, M. (2006). Vibration characteristics of laminated composite plates with embedded shape memory alloys. *Composite Structures*, 74(4), 389–398.
- Zhao, H., & Cao, D. (2013). A study on the aero-elastic flutter of stiffened laminated composite panel in the supersonic flow. *Journal of Sound and Vibration*, 332(19), 4668-4679.
- Zhao, S., Teng, J., Wang, Z., Sun, X., & Yang, B. (2018). Investigation on the Mechanical Properties of SMA / GF / Epoxy Hybrid Composite Laminates : *Materials*, 11(2), 246.

Zhou, G., & Lloyd, P. (2009). Design, manufacture and evaluation of bending behaviour of composite beams embedded with SMA wires. *Composites Science and Technology*, 69(13), 2034–2041.

Zhou, W., Wentz, T., Liu, D., Mao, X., Zeng, D., Torab, H., Dahl, J., & Xiao, X. (2020). A comparative study of a quasi 3D woven composite with UD and 2D woven laminates. *Composites Part A: Applied Science and Manufacturing*, 139, 106139.



APPENDICES

Appendix A1. Calculation of volume fraction of constituents of composite structures for tensile test

$m_c = 8.36\text{gm}$, $m_f = 6.29\text{gm}$, $\rho_f = 2.54\text{gm/cm}^3$, $\rho_m = 1.1\text{gm/cm}^3$, $m_{SMA} = 0.108\text{gm}$, $\rho_{SMA} = 6.45\text{ gm/cm}^3$,

For matrix weight,

$$m_c = m_f + m_m + m_{SMA}$$
$$m_m = 1.962\text{gm}$$

1. Fibre volume fraction

$$V_f(\%) = \frac{m_f * \rho_c}{m_c * \rho_f} * 100$$

For calculating density,

$$\rho_c = \frac{m_c}{m_c - m_w} * 0.997$$

Dimensions of composite sample for calculating density are $2 \times 2 \times 0.07\text{cm}^3$ while dry weight and weight in water are $m_c = 0.540\text{ gm}$ and $m_w = 0.262\text{ gm}$.

$$\rho_c = \frac{0.540}{0.540 - 0.262} * 0.997 = 1.937\text{gm/cm}^3$$

$$V_f(\%) = \frac{6.29 * 1.937}{8.36 * 2.54} * 100 = 57.38(\%)$$

2. Matrix volume fraction

$M_m = 1.962\text{ gm}$,

$$V_m(\%) = \frac{m_m * \rho_c}{m_c * \rho_m} * 100$$

$$V_m(\%) = \frac{1.962 * 1.937}{8.36 * 1.1} * 100 = 41.33\%$$

3. SMA volume fraction

$$V_{SMA}(\%) = \frac{m_{SMA} * \rho_c}{m_c * \rho_{SMA}} * 100$$

$$V_{SMA}(\%) = \frac{0.108 * 1.937}{8.36 * 6.45} * 100 = 0.388\%$$

4. Void Content (%)

$$V_v(\%) = 100 - (V_f(\%) + V_m(\%) + V_{SMA}(\%))$$

$$V_v(\%) = 100 - (57.38 + 41.33 + 0.388) = 0.902\%$$

Appendix A2. Calculation of volume fraction of constituents of composite structures for modal analysis and aeroelastic analysis

$m_c = 20.055\text{gm}$, $m_f = 15.15\text{gm}$, $\rho_f = 2.54\text{gm/cm}^3$, $\rho_m = 1.1\text{gm/cm}^3$, $m_{SMA} = 0.26\text{gm}$,
 $\rho_{SMA} = 6.45\text{ gm/cm}^3$,
 For matrix weight,

$$m_c = m_f + m_m + m_{SMA}$$

$$m_m = 4.645\text{gm}$$

1. Fibre volume fraction

$$V_f(\%) = \frac{m_f * \rho_c}{m_c * \rho_f} * 100$$

$$\rho_c = \frac{m_c}{m_c - m_w} * 0.997$$

Dimensions of composite sample for calculating density are $2 \times 2 \times 0.07\text{cm}^3$ while dry weight and weight in water are $m_c = 0.544\text{ gm}$ and $m_w = 0.264\text{ gm}$.

$$\rho_c = \frac{0.544}{0.544 - 0.264} * 0.997 = 1.937\text{gm/cm}^3,$$

$$V_f(\%) = \frac{15.15 * 1.937}{20.055 * 2.54} * 100 = 57.61(\%)$$

2. Matrix volume fraction

$$M_m = 1.962\text{ gm}$$

$$V_m(\%) = \frac{m_m * \rho_c}{m_c * \rho_m} * 100$$

$$V_m(\%) = \frac{4.645 * 1.937}{20.055 * 1.1} * 100 = 40.78\%$$

3. SMA volume fraction

$$V_{SMA}(\%) = \frac{m_{SMA} * \rho_c}{m_c * \rho_{SMA}} * 100$$

$$V_{SMA}(\%) = \frac{0.26 * 1.937}{20.055 * 6.45} * 100 = 0.389\%$$

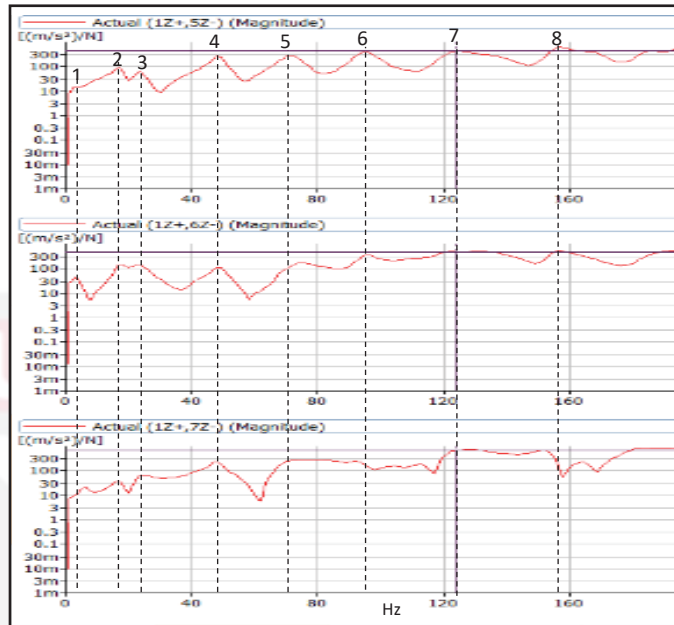
4. Void Content (%)

$$V_v(\%) = 100 - (V_f(\%) + V_m(\%) + V_{SMA}(\%))$$

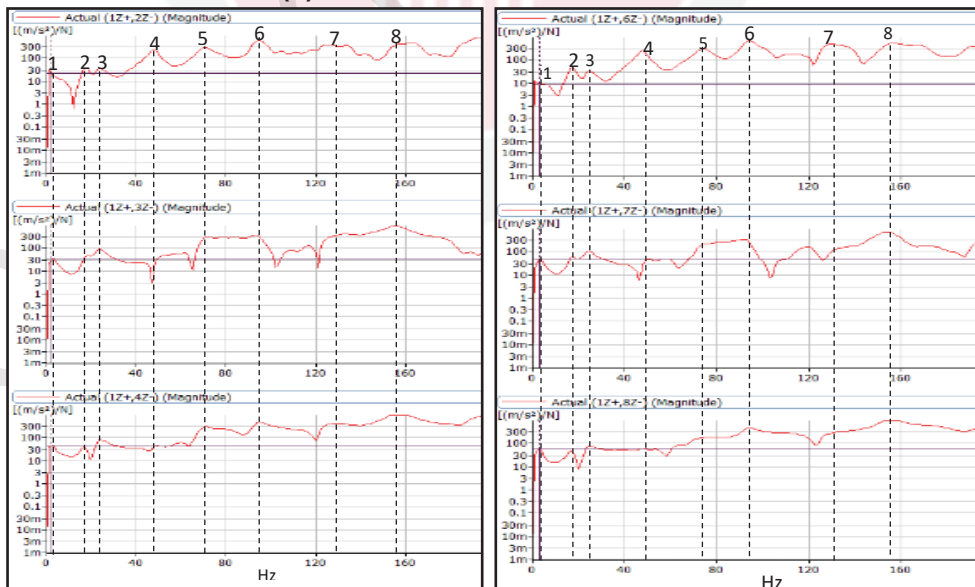
$$V_v(\%) = 100 - (57.61 + 40.78 + 0.389) = 1.221\%$$

Appendix B1

Appendix B1.1. FRF plot of L2L without SMA wire



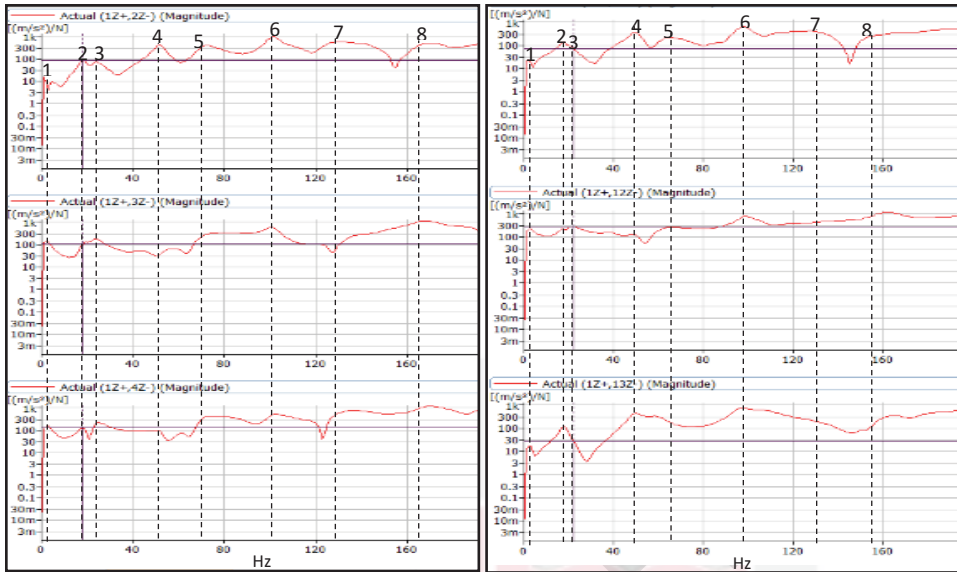
Appendix B1.2. FRF plot of L2L with SMA wire at mid (a) Inactive SMA wire (b) Activated SMA wire



a

b

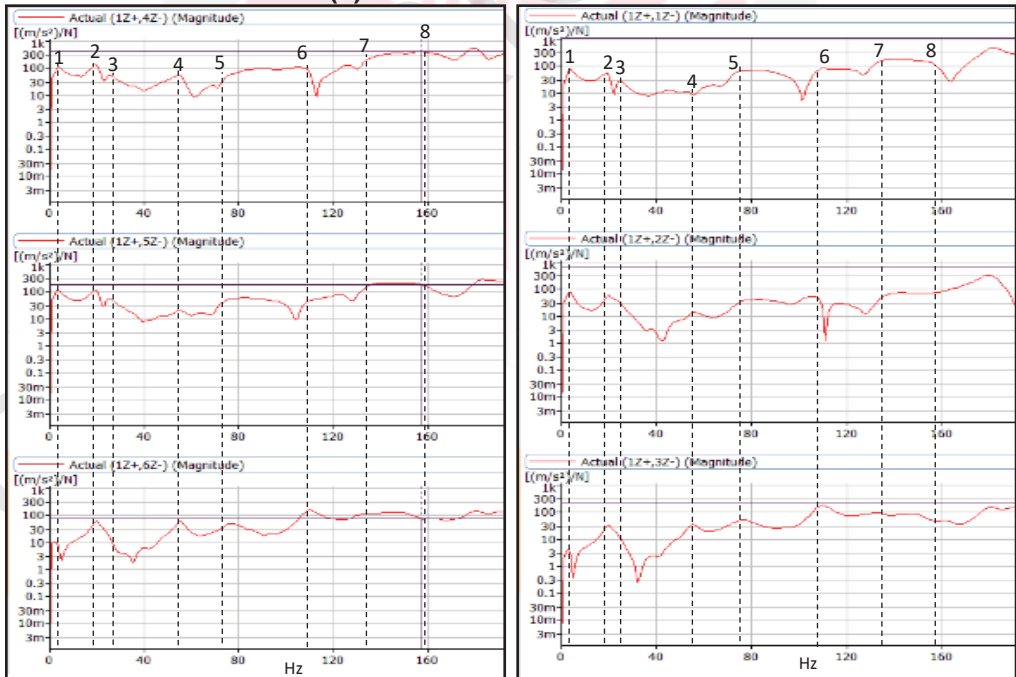
Appendix B1.3. FRF plot of L2L with SMA wire at near to trailing edge (a) Inactive SMA wire (b) Activated SMA wire



a

b

Appendix B1.4. FRF plot of L2L with SMA wire at leading edge (a) Inactive SMA wire (b) Activated SMA wire

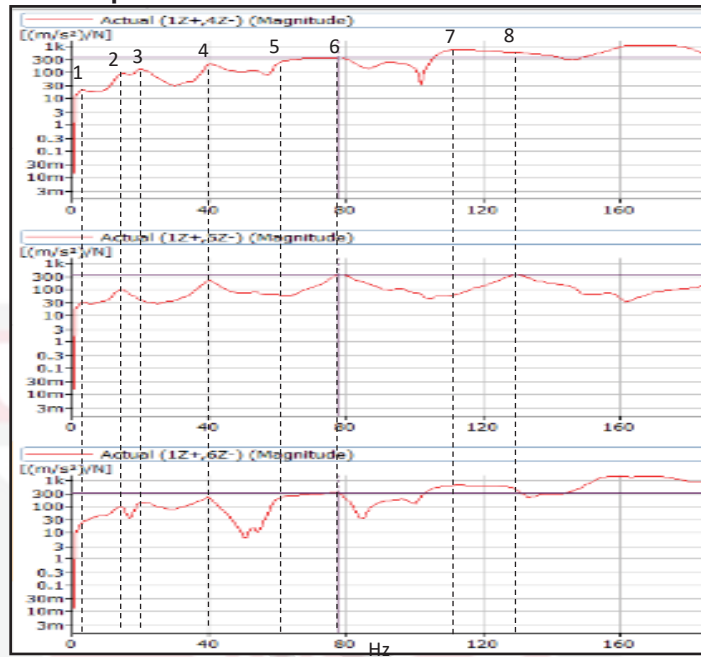


a

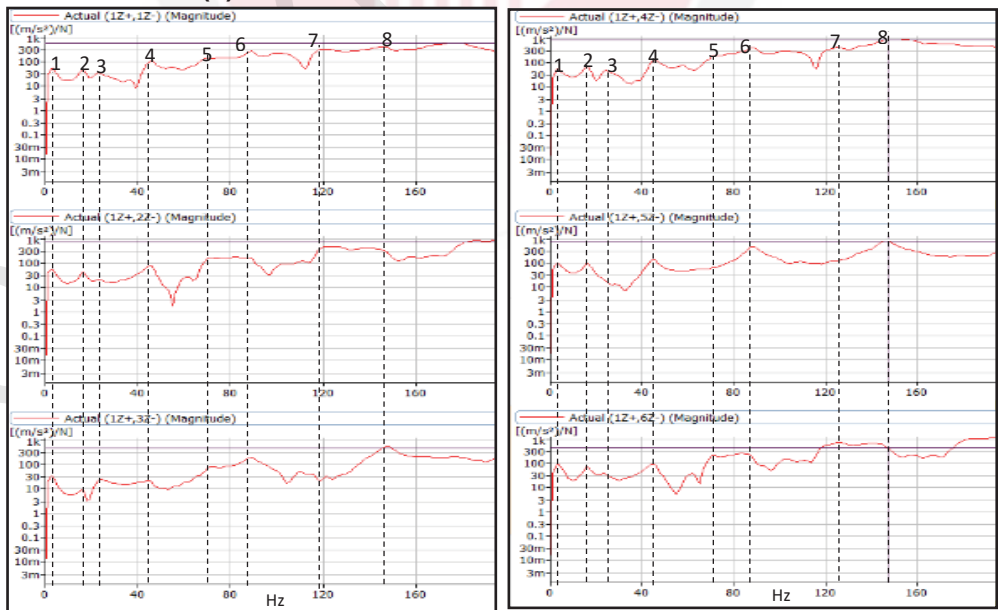
b

Appendix B2

Appendix B2.1. FRF plot of TT without SMA wire



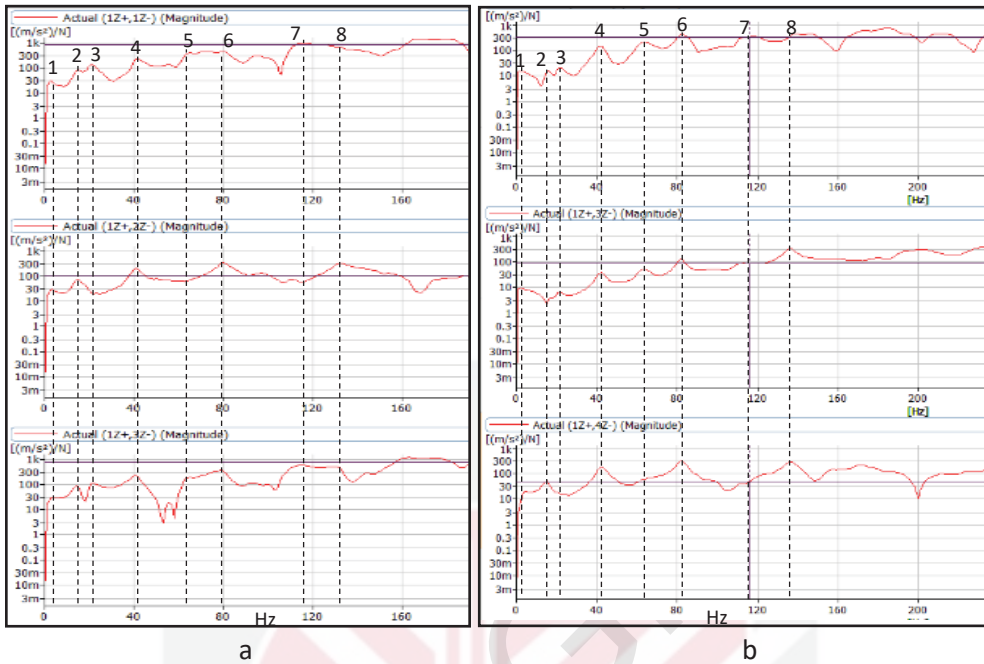
Appendix B2.2. FRF plot of TT with SMA wire at mid (a) Inactive SMA wire (b) Activated SMA wire



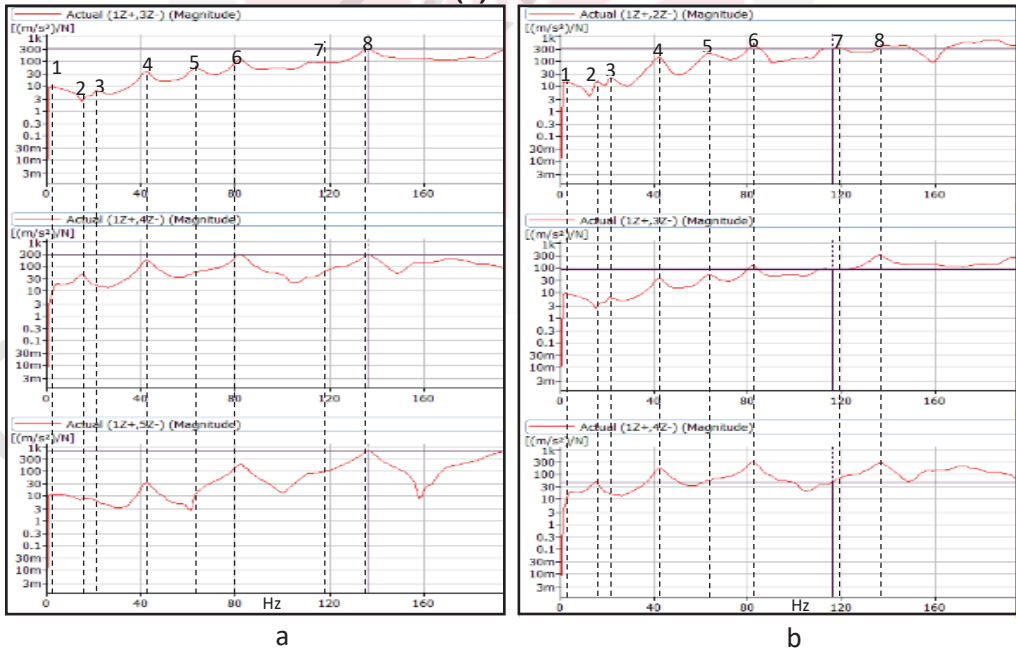
a

b

Appendix B2.3. FRF plot of TT with SMA wire at near to trailing edge (a) Inactive SMA wire (b) Activated SMA wire

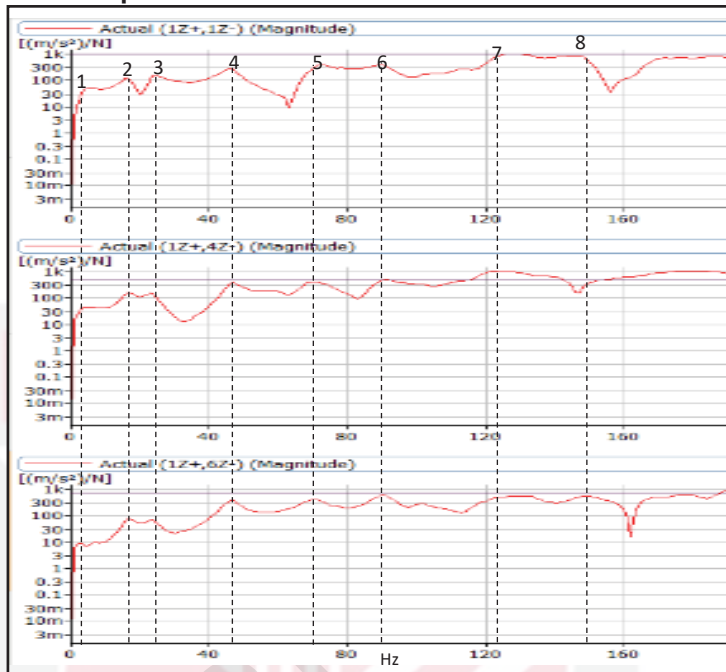


Appendix B2.4. FRF plot of TT with SMA wire at near to leading edge (a) Inactive SMA wire (b) Activated SMA wire

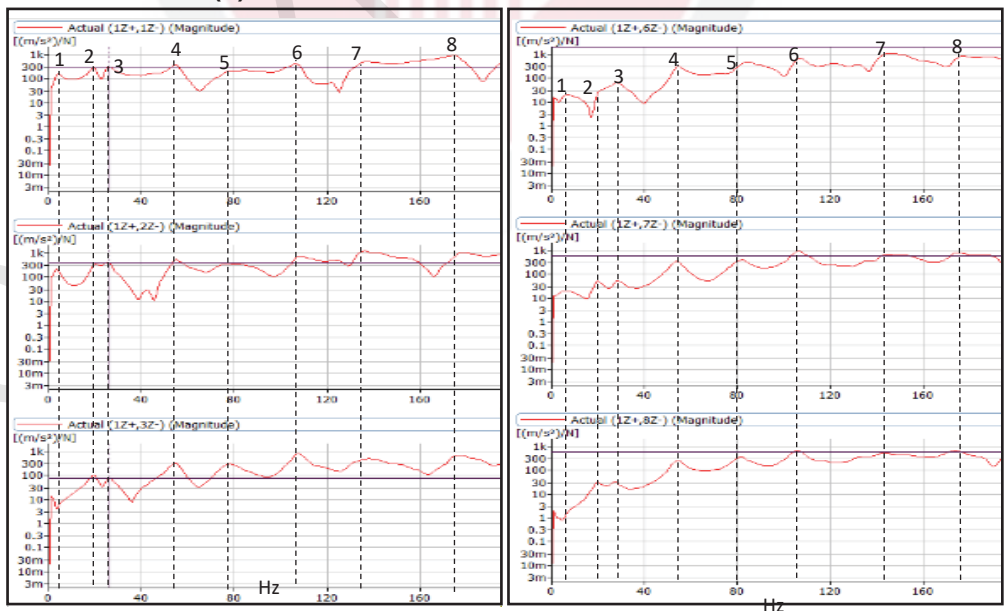


Appendix B3

Appendix B3.1. FRF plot of MF without SMA wire



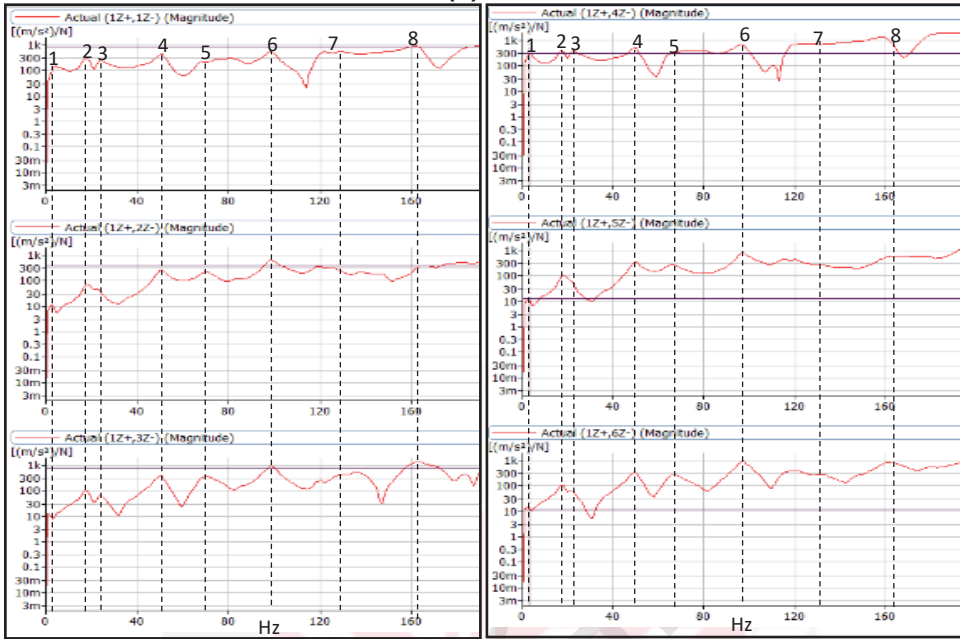
Appendix B3.2. FRF plot of MF with SMA wire at mid (a) Inactive SMA (b) Active SMA



a

b

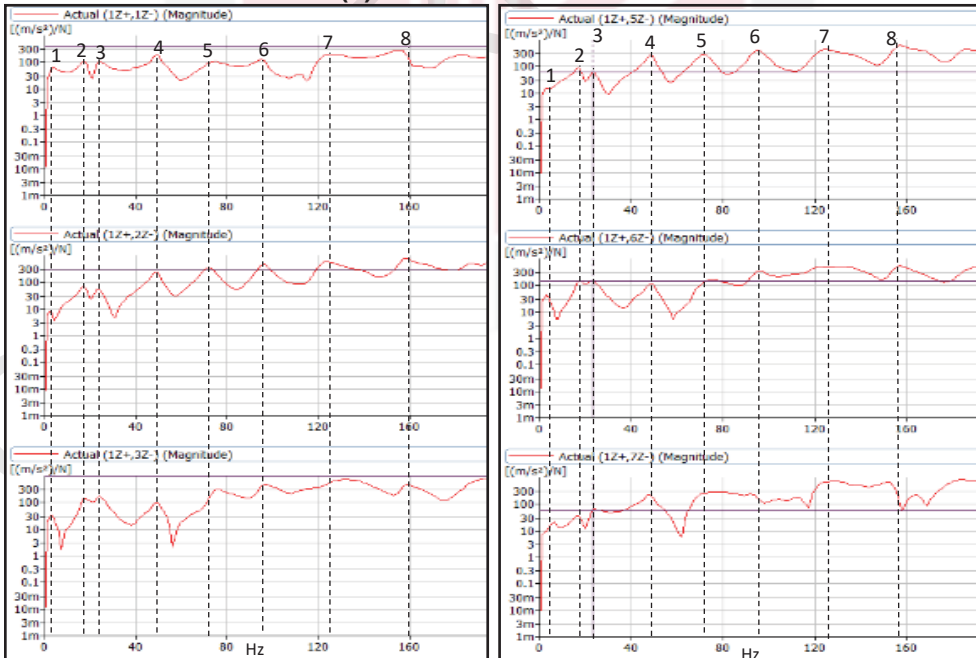
Appendix B3.3. FRF plot of MF with SMA wire at near to trailing edge (a) Inactive SMA wire (b) Activated SMA wire



a

b

Appendix B3.4. FRF plot of MF with SMA wire at leading edge (a) Inactive SMA wire (b) Activated SMA wire



a

b

Appendix C1

Appendix C1. Calculations of bending moments of 3D woven L2L with inactive and activated SMA wire at mid

i) 3D woven L2L with inactive SMA wire at mid:

Length of the cantilevered composite plate= $L = 0.3$ m,

Young's Modulus of 3D woven L2L with inactive SMA wire (calculated in section 4.2.3)= $E = 15.78$ GPa

$$I = bh^3/12 = 1.43 \times 10^{-12} \text{ m}^4,$$

The aerodynamic loading is mainly depend on pressure of airflow and it is mainly responsible for bending of plate. Weight of the plate and other factors are neglected as these are same for inactive and activated SMA wire. So the load distributed to the plate is $w_1 = P * L$.

$$\text{The Dynamic pressure of the airflow} = P = \frac{1}{2} \rho_{\text{air}} U^2$$

Speed of air for maximum deflection of plate before flutter phenomenon is U (From Figure 4.22(b))= 5.98 m/sec

Density of the air= $\rho = 1.225$ kg/m³.

$$\text{The Dynamic pressure of the airflow} = P = \frac{1}{2} \rho_{\text{air}} U^2 = 21.90 \text{ N/m}^2$$

And the load distributed to the plate is $w_1 = P * L = 6.57$ N/m.

The bending moment at the tip of the cantilevered plate with inactive SMA wire (Equation 3.7) $M_1 = -\frac{w_1 L^2}{6} = -0.0986$ Nm

The negative sign of the moment shows that the bending of the plate is in the downward direction.

The maximum deflection of the tip of the plate calculated (Equation 3.8)

$$= d_1 = \frac{w_1 L^4}{30EI} = 0.0786 \text{ m}$$

ii) **3D woven L2L with activated SMA wire:**

Young's Modulus of 3D woven L2L with activated SMA wire (section 4.2.3)=
 $E=21.29 \text{ GPa}$

$$I = bh^3/12 = 1.43 \cdot 10^{-12} \text{ m}^4$$

Maximum deflection of the tip of the plate calculated from strain (Equation 3.9),

$$d = \frac{2L^3}{3hx} (\epsilon) = 0.0789 \text{ m}$$

Speed of air before flutter phenomenon for maximum deflection of the plate is

$$U(\text{From Figure 4.22(c)}) = 5.40 \text{ m/sec}$$

Density of air is $\rho = 1.225 \text{ kg/m}^3$,

$$\text{The Dynamic pressure of the airflow} = P = \frac{1}{2} \rho_{\text{air}} U^2 = 17.86 \text{ N/m}^2$$

The load distributed to the plate due to airflow is $w_1 = P \cdot L = 5.358 \text{ N/m}$.

$$'w_2' \text{ is calculated by rearranging equation Equation 3.13 } (d = \frac{w_1 L^4}{30EI} + \frac{11w_2 L^4}{120EI})$$

and putting values of d , w_1 , L , E , and I .

$$w_2 = 1.286 \text{ N/m}.$$

Now Bending moment at the tip of the plate with activated SMA wire (Equation 3.12) = $M = \frac{w_1 L^2}{6} + \frac{w_2 L^2}{3} = 0.1187 \text{ Nm}$.

So the bending moment of the plate with activated SMA wire is 20.39 % higher than the bending moment of the plate without activating the SMA wire.

BIODATA OF STUDENT

Danish Mahmood Baitab was born on 1st September, 1988 in Rawalakot, District Poonch, Azad Jammu and Kashmir, Pakistan. After completing his higher secondary education, he went to National Textile University Faisalabad, Pakistan. He completed his Bachelor's degree in "Textile Engineering" specialization of "Fabric Manufacturing" in 2012. He did his Master's degree in "Advanced Materials Engineering in 2015 from National Textile University Faisalabad, Pakistan. He joined National Textile University as a Lecturer in November 2012 and served five years. He was awarded a foreign scholarship by Higher Education Commission, Islamabad, Pakistan for PhD studies in 2017. Pursuing this, he took admission in the Department of Aerospace Engineering, University Putra Malaysia under the supervision of Associate Professor Dr. Dayang Laila Abang Abdul Majid, Dr. Ermira Junita Abdullah and Dr. Mohd Faisal Abdul Hamid.

LIST OF PUBLICATIONS

- Baitab, D.M., Majid, D. L. A., Abdullah, E. J., & Hamid, M. F. A. (2018). A review of techniques for embedding shape memory alloy (SMA) wires in smart woven composites. *International Journal of Engineering and Technology*, 7(4), 129-136.
- Baitab, D.M., Majid, D. L. A., Abdullah, E. J., & Hamid, M. F. A. (2020). Improving the stiffness of multilayer 3D woven composites by the integration of shape memory alloys (SMAs) into structures. *The Journal of The Textile Institute*, 111(9), 1371–1379.
- Baitab, D.M., Majid, D. L. A, Abdullah, E. J., & Hamid, M. F. A. (2020). Tensile behavior of multilayer 3D smart woven composites embedded with shape memory alloy (SMA) wires. *Journal of Materials Research and Technology*, 9(5), 10876–10885.



UNIVERSITI PUTRA MALAYSIA

**STATUS CONFIRMATION FOR THESIS / PROJECT REPORT
AND COPYRIGHT**

ACADEMIC SESSION : Second Semester 2020/2021

TITLE OF THESIS / PROJECT REPORT :

**AEROELASTIC FLUTTER PERFORMANCE OF SHAPE MEMORY ALLOY-
EMBEDDED 3D WOVEN COMPOSITE PLATE UNDER SUBSONIC FLOW**

NAME OF STUDENT :

DANISH MAHMOOD BAITAB

I acknowledge that the copyright and other intellectual property in the thesis/project report belonged to Universiti Putra Malaysia and I agree to allow this thesis/project report to be placed at the library under the following terms:

1. This thesis/project report is the property of Universiti Putra Malaysia.
2. The library of Universiti Putra Malaysia has the right to make copies for educational purposes only.
3. The library of Universiti Putra Malaysia is allowed to make copies of this thesis for academic exchange.

I declare that this thesis is classified as:

*Please tick (✓)

CONFIDENTIAL

(Contain confidential information under Official Secret Act 1972).

RESTRICTED

(Contains restricted information as specified by the organization/institution where research was done).

OPEN ACCESS

I agree that my thesis/project report to be published as hard copy or online open access.